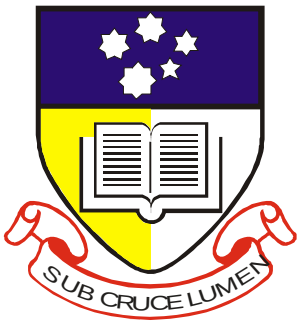

DESIGN OF AN ADAPTIVE DYNAMIC VIBRATION ABSORBER

Christopher Ting-Kong

Department of Mechanical Engineering

The University of Adelaide

South Australia 5005

Thesis submitted for the degree of

Master of Engineering Science on the 21st April, 1999.

DESIGN OF AN ADAPTIVE DYNAMIC VIBRATION ABSORBER

TABLE OF CONTENTS

LIST OF FIGURES

Notation

m_a = mass of absorber or secondary structure (kg)

m_b = mass of base or primary structure (kg)

ω_a = natural frequency of absorber (rad/s)

$\omega_{b,}$ ω_n = natural frequency of base (rad/s)

$\omega_{11,}$ ω_{22} = first and second modes of the composite system (rad/s)

p = excitation or operating frequency (rad/s)

E = modulus of elasticity (Pa)

I = second moment of inertia (m^4)

ρ = density (kg/m^3)

H_a = impedance of absorber (N/m/s)

H_b = impedance of base (N/m/s)

u_b = maximum displacement of base with absorber attached (m)

u_F = maximum displacement of base without absorber attached (m)

DESIGN OF AN ADAPTIVE DYNAMIC VIBRATION ABSORBER

ABSTRACT

The aim of this thesis is to investigate the use of a Dynamic Vibration Absorber to control vibration in a beam. Traditional means of vibration control have involved the use of passive and more recently, active methods. This study is different in that it involves an adaptive component in the design of vibration absorber using two novel designs for the adaptive mechanism.

The first design incorporates the use of an enclosed air volume to provide the variable stiffness component in the absorber. By adjusting the volume of compressible air within the absorber, the stiffness characteristics of the absorber can be altered, enabling the device to adapt to changing vibration frequencies. Work here includes a theoretical investigation of the device. Following this, two prototypes are constructed and tested, the second of which is the refined model used for further testing.

The second design incorporates the use of two concentrated masses cantilevered from two rods. The adaptive solution is achieved by moving the two masses along the length of the rod, producing a changing natural frequency for the absorber device. An analytical model of this device is developed as well as a finite element model. Results from both are compared to those obtained experimentally.

Finally, a tuning algorithm is derived for the second absorber, and a control system constructed to make the dynamic vibration absorber “adaptive”. Experiments are undertaken to determine the effectiveness of the absorber on the beam subject to changing excitation frequencies. The outcome of this research is that an Adaptive Vibration Absorber has been constructed with a computer interface such that the device can be used “on line”.

STATEMENT OF ORIGINALITY

This thesis does not contain any material which has been accepted for the award of any degree or diploma in this university or other tertiary institution. Unless where stated or referenced, this work contains no material which has been previously published or written by other researchers.

Permission is given by the author to the relevant bodies within the University of Adelaide, for purposes of photocopying and reproduction, and its availability for loan.

Signed:…….. Date:……

ACKNOWLEDGMENTS

The author would like to thank Dr. Scott D Snyder for his supervision and input, and his willingness to support the ideas forwarded in the research.

Thanks must also go to Dr. Colin H. Hansen for his interest and comments in the discussion of the work. The study would never have been possible without the talents and suggestions from George Osborne, Silvio De Ieso, Alan Mittler and Derek Franklin.

The author would also like to thank Ron Jager, Craig Price and Malcolm Bethune for all their work in the construction of the absorbers.

Finally, a big thank you to all the administration staff in the department of mechanical engineering, and my fellow cubicle peers, and also in particular, Benny B. Cazzolato, for much of his intelligent input.

CHAPTER 1. INTRODUCTION AND LITERATURE REVIEW

1.1 INTRODUCTION

When a structure is undergoing some form of vibration, there are a number of ways in which this vibration can be controlled. *Passive* control involves some form of structural augmentation or redesign, often including the use of springs and dampers, that leads to a reduction in the vibration. *Active* control augments the structure with sensors, actuators and some form of electronic control system, which specifically aim to reduce the measured vibration levels.

This research investigates the use of *Adaptive Tuned Dynamic Vibration Absorbers* (ATDVA) to control vibration in a structure. A dynamic vibration absorber (DVA) is essentially a secondary mass, attached to an original system via a spring and damper. The natural frequency of the DVA is tuned such that it coincides with the frequency of unwanted vibration in the original system. This results in a subcomponent of the total structure adding a large input impedance to the primary structure, thus '*absorbing*' the inertial energy transferred from the primary structure. *Active* DVAs are characterised by a secondary mass, mounted to a vibratory primary system, that is directly connected to an actuator and electronic control system. However, *Adaptive Tuned* refers to the ability of the DVA to change its internal *properties* to reflect changes in the vibratory environment.

The use of DVAs is advantageous because of their mobility, and their ability to be incorporated into the structure after the design stage. This often allows for the absorber to be mounted without affecting the mounting between the structure and the supporting foundation, therefore providing a rigid mount with minimal movement. Other advantages of DVAs over *active* attenuation techniques include the ability to guarantee stability, low cost, low power, and simplicity of implementation.

This research will also investigate the *effectiveness* of ATDVA, especially as an alternative to active vibration control. DVAs can be constructed using a variety of different mechanisms and orientations; this study proposes two different arrangements.

The first chapter reviews the theoretical model of the DVA, and concepts relating to the testing of the devices. A review of past research in this area is also undertaken. The second chapter details work undertaken on the first DVA arrangement used in this study. This absorber is based on the idea of using an enclosed air volume to provide a variable stiffness component. The third chapter details a second arrangement of an adaptive dynamic vibration absorber, one based on the concept of a variable length cantilevered beam. The fourth chapter summarises the work which has been completed in this study and discusses possible areas of improvement for both absorbers.

1.2 LITERATURE REVIEW

1.2.1 Existing Technology and Prior Research

Active Dynamic Vibration Absorbers

Dynamic Vibration Absorbers were first invented in 1909 (Den Hartog, 1956). Work on DVAs was undertaken rigorously during the development of helicopter rotor blades after 1963 (Flannelly, 1963, Jones, 1971), and more recently, for the defence mechanism against earthquakes. Much work has been directed towards the use of DVAs attached to building structures, to counter seismic movements and wind forces. In recent studies, interest has also been focused on the use of feedback and feedforward control systems, and the synthesis of DVAs for multiple-degree-of-freedom systems.

Yoshida K. *et al.* (1988) examined the combined use of both feedforward and feedback control to attenuate both stationary and non-stationary (random) inputs, with an active DVA. Yoshida used a linear motor controlled digitally using optimal feedback and feedforward links, to actuate the absorbing mass. DVAs have the advantage in that the controller is able to guarantee a closed-loop stability, even with minimal knowledge of the controlled system (Lee-Glauser, 1995).

Harris and Crede (1961) provide a description of a number of different DVA arrangements, including pendulum and linear spring-mass arrangements. Description is also given of a tube form, in which a fluid rolls from one tank to another, often used for antiroll in ships. Absorber systems can include rotational or linear motion, or both. As this study focuses on the design of a suitable and controllable DVA, it is favourable to restrict the research to single-degree of freedom linear systems.

Hunt (1979) outlines many applications where ADVAs have been useful. In the area of helicopter rotor blade development, hydraulic Active Dynamic Absorbers have found use. Here, a double-acting hydraulic cylinder is placed between the rotor and the fuselage, the rotor being the absorber mass. Two feedback signals are taken from the rotor and the fuselage through an amplifier, which sends a control signal to a servo valve. This valve then controls the hydraulic actuator.

Active Vibration Absorbers have also been used for suppressing vibration in beams which have multiple resonant frequencies. Passive dynamic absorbers can be effective only for a single resonance frequency, and may not be effective at other resonant frequencies or for modes where a node is present at the location of the absorber. A *force generator* developed by Rockwell (1965) also acting as the absorber mass can be mounted on the beam. A sensor mounted on the other side of the beam detects the motion of the beam and sends a feedback signal to the generator, which in turn reacts against the motion of the vibration.

Another field is in the control of tower structures. Korenev et al. (1995) details a number of different designs of dynamic absorbers for structural applications.

Adaptive-Passive Dynamic Vibration Absorbers

Numerous applications involving active control of Dynamic Absorbers have dealt with actuating the absorber mass directly. **This study is different in the way that the "active" component is implemented. Here, the actuator will be controlling the stiffness of the spring, thus controlling the natural frequency of the absorber system (the secondary system).** This method of control has the potential to be less energy consuming, as the power required to adjust the spring variable is expected to be less than the power required to actuate the mass directly. This method is best described as an adaptive-passive approach to vibration control.

Adaptive-passive methods involve the use of passive elements which can be optimally tuned to perform over a certain frequency range. Unlike a fully active system, this form of control cannot add "negative" damping to an existing system (ie. the poles of the system cannot migrate across the imaginary axis). Thus a system which is already stable can not be made unstable through the use of this method. Adaptive Helmholtz resonators, described by Lamancusa (1987), are an example of where adaptive-passive methods have been used for narrowband applications. These resonators are able to control sound within a certain frequency range, over a number of different speeds, by varying the resonator neck dimensions or cavity volume or both. In the area of broadband applications, Graf et al (1987) explains the use of adaptive-passive methods to vary the stiffness and damping of an engine mount.

In the area of structural control, Ryan et al (1994) designed an adaptive-passive vibration absorber using a variable spring as the adaptive component. The stiffness was controlled using a spring inserted through a sliding plate, which could then be moved to alter the effective number of coils in the spring, which in turn affected the overall stiffness of the spring. The plate was moved according to the feedback signal linked an accelerometer, mounted on the primary vibratory system.

The physical limitation of damping present in all systems of dynamic absorbers, and the limitations of the electrical properties in the equipment, resulted in some residual motion present in the vibratory structure. However, the results from this study indicated that the use of adaptive-passive vibration absorbers is feasible in the control of vibration.

Self-adapting absorbers have been previously used in the vibration control of unbalanced rotating shafts. These come in the form of centrifugal absorbers, which can vary their pendulum angle in accordance with the angular speed. This results in the stiffness of the absorber increasing at a rate square to the angular speed, which means the eigenfrequency increases directly with the speed of the rotating shaft.

1.2.2 Summary of contribution to current knowledge addressed by this thesis

The main objective of this work is to examine the use of two different arrangements as adaptive dynamic vibration absorbers.

Adaptive dynamic vibration absorbers are essentially a subset of those in active control (for vibration and structural/acoustic control), with particular emphasis on tonal disturbances. Where they can be used, DVAs have a distinct advantage in guaranteed stability. This study will aim to develop a dynamic vibration absorber with variable stiffness that is:

1. Practical (construction from common materials, portability, and easy to use)
2. Has a “broad” operating frequency range
3. Low Cost
4. Low power consumption

Firstly, the effectiveness of using enclosed air as a means of providing the stiffness for an adaptive-tuning DVA will be investigated. Secondly, the usefulness of using cantilevered beams with concentrated end-masses will also be investigated as a second mechanism. A design procedure for the tuning algorithm for the absorber will be derived.

1.2.3 Strategies taken here to achieve the objectives

1. Determine appropriate absorber sizes by experimentation with an existing vibrating structure assembly; investigate the potential of various absorber models, and devices which will enable adjustment of the absorber stiffness. Determine the frequency range over which the absorber will be useable.

2. Build a prototype model of an absorber with a variable enclosed air volume and test its effectiveness for a single resonance frequency. An analytical procedure will be used to design a DVA resonating at a low frequency (less than 50) Hz. It is expected that the sealing the air volume will be critical, as this will determine whether sufficient stiffness can be provided without pressurising the air itself. Minimal damping is often recommended for an absorber, as excessive damping will limit the single-frequency attenuation in exchange for expanded bandwidth. This may be a problem with an “air” device.

3. Test the effectiveness of the prototype absorber within a given frequency range. Determine the sensitivity of the absorber to variations in the excitation frequency.

4. Construct an actuator that can control the stiffness of a mechanical spring component, and derive algorithms for the control system. Undertake experimental tests and compare the results with theoretical data.

5. Verify the usefulness of this second absorber arrangement, by subjecting it to successive excitation signals of changing frequency.

1.2.4 Analysis of the Dynamic Vibration Absorber

The analytical model of the absorber will be assumed to be a spring-mass system (although minimal damping will always be present in the real form). The overall system is represented in figure 1.1.

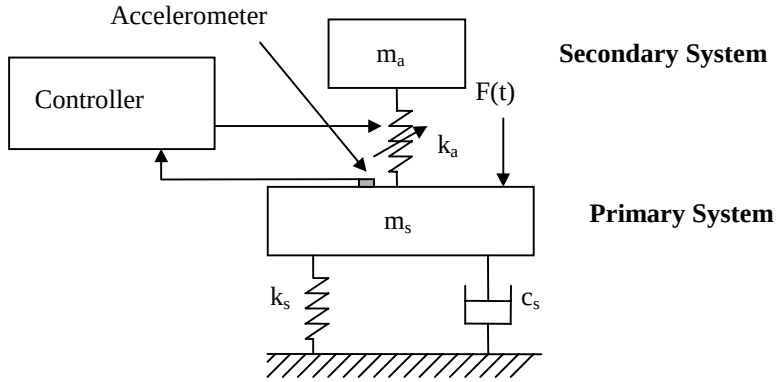

Figure 1.1 Representation of an Adaptive Vibration Absorber

The range of frequencies over which the study is conducted has been chosen to be $\omega_n \in [30,100]$ Hz. This range has been selected because of the vast number of 'real' vibration problems, which occur within it, particularly in relation to problems associated with rotating machinery. It is also a range where the use vibration absorbers may be preferable to other passive treatments, such as constrained layer damping, owing to size and performance requirements.

For a single degree of freedom system, when an absorber with natural frequency ω_n is attached to a system, a transmission zero, or "antiresonance" in the resulting system response is found at this natural frequency.

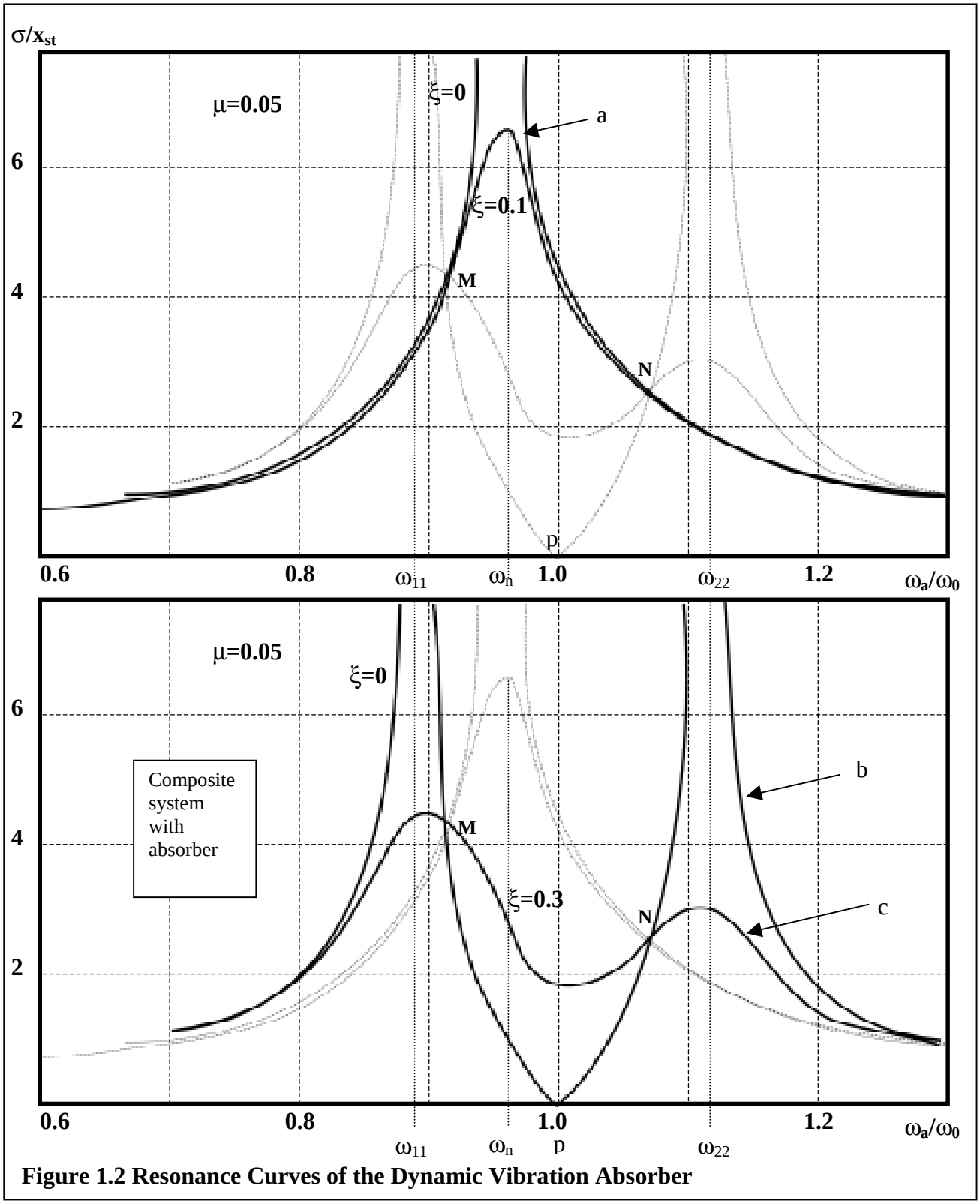

Figure 1.2 Resonance Curves of the Dynamic Vibration Absorber

Illustrated in figure 1.2 is a typical frequency response of the primary system (a) and the composite system including a dynamic absorber (b). The amplitude values are the ratio between acceleration levels σ taken from the primary system and the input levels x_{st} entering the primary system. When an absorber with a natural frequency ω_n is attached to the system, the single resonance peak of the primary system is replaced by two resonances on either side of the original resonance; the original resonance has now been replaced by an antiresonance. This basic physical behavior has great practical potential. For example, if excitation is provided by machinery operating near frequency ω_n, vibration can be reduced by attaching the absorber so that an antiresonance p, is created near that frequency.

Observe from curve (b) in the lower plot in figure 1.2 that the combined primary system and absorber has two resonance peaks, placed in frequency on either side of the absorber-induced antiresonance. The greater the ratio μ of absorber mass to the system mass, the further apart the resonance frequencies ω_{11} and ω_{22} will be. Typical values for the absorber mass to primary mass ratio, μ, range from 0.1 to 1.0. For smaller values of μ, the sensitivity of the absorber to tuning increases.

Line (c) shows the effects of damping within the absorber. With damping present, the level of attenuation is less at the resonance frequency, p, but the range over which attenuation in the vibration response is provided is now increased. The optimal amount of damping present in the absorber system is achieved when the points M and N are at equal amplitudes. All the resonance curves for a dynamic absorber pass through these two points. For damping which is excessive, however, it is possible for the absorber to move in phase with the primary structure, thus increasing its amplitude.

1.2.5 Analysis of Vibration in Base Structure - Simply Supported Beam

The experimental tests to be discussed later in this thesis are undertaken on a simply supported rectangular cross-section beam. The resonance frequencies of the modes of the beam are adjusted by adjusting the axial position of the supports. This is illustrated in figure 1.3.

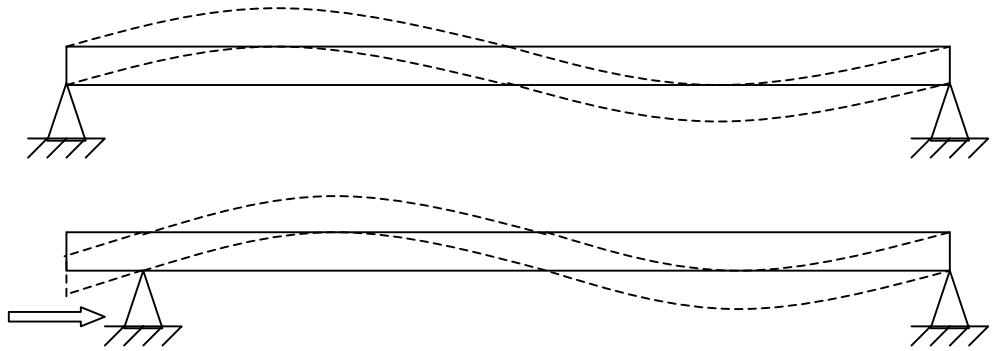

The natural frequencies of the beam are adjusted by moving the axial location of the supports.

Figure 1.3 Changing the natural frequency of a beam

The purpose of constructing the test rig such that its resonance frequencies can be adjusted is to test the effectiveness of the absorber over a range of frequencies. When the absorber is mounted on the beam, the resonance of the beam will be adjusted such that the **span** in which the absorber is operating will be within the same proximity as the resonant modes of the beam. This procedure will also allow for the different absorber prototypes (which are constructed for different operating ranges) to be tested on the same rig.

1.2.6 Governing Equations for Base Structure

The governing equation for the natural frequency of a simply supported beam is given by (Thomson):

$$\omega_n = \beta_n^2 \sqrt{\frac{EI}{\rho A}}$$
$$= (\beta_n l)^2 \sqrt{\frac{EI}{\rho A l^4}}$$

For the rectangular uniform beam, E = 207 x 10^9 Pa, ρ = 7800 kg/m^3.

The second moment of inertia, I = (bh^3)/12.

The value $(\beta l)^2$ depends on the boundary conditions of the beam. Typical end conditions are given in the table 1.1 below (Thomson).

Table 1.1

Beam Configuration	$(\beta_1 l)^2$	$(\beta_2 l)^2$	$(\beta_3 l)^2$
Simply Supported	9.87	39.5	88.9
Cantilever	3.52	22.0	61.7
Free-Free	22.4	61.7	121.0
Clamped-Clamped	22.4	61.7	121.0
Clamped-Hinged	15.4	50.0	104.0
Hinged-Free	0	15.4	50.0

For a beam, b = 0.025m, h = 0.05m, l = 1.135m (initial setup of the test rig),

$$I = \frac{0.025 \times 0.05^3}{12}$$
$$= 2.6 \times 10^{-7} m^4$$

For a simply supported beam, $(\beta l)^2 = 9.87$ for the fundamental mode.

$$\omega_n = 9.87 \sqrt{\frac{207 \times 10^9 \times 2.6 \times 10^{-7}}{7800 \times 1.25 \times 10^{-3} \times 1.135^4}}$$
$$= 402 rad/s$$
$$\therefore f = 64 Hz$$

For a free-free beam, $(\beta l)^2 = 22.4$ for the fundamental mode

$$\omega_n = 22.4 \sqrt{\frac{207 \times 10^9 \times 2.6 \times 10^{-7}}{7800 \times 1.25 \times 10^{-3} \times 1.135^4}}$$
$$= 1290 rad/s$$
$$\therefore f = 206 Hz$$

The value obtained from experimental procedures should lie in between clamped-clamped and simply supported value, as the end conditions of the actual beam are somewhere between the two.

CHAPTER 2 DYNAMIC VIBRATION ABSORBER USING ENCLOSED AIR

2.1 INTRODUCTION

This chapter considers the design of a dynamic vibration absorber with a variable air volume backing. The following work is undertaken:

1. Conceptual design of a first prototype is done to test the physical mechanism of using air as a variable spring component.
2. A second prototype is constructed to address the problems found in the first prototype. The amount of variation in stiffness is investigated for this mechanism.
3. The second prototype is tested, and further refinement is made to this design.
4. Results from the tests are analysed.

2.2 FIRST PROTOTYPE

The first absorber proposed here can be explained with reference to figure 2.1. The impetus behind the concept is that for some applications (particularly vehicle applications), the absorber must be as light as possible. To be of practical use, the design must incorporate a means of adjusting the absorbing frequency; since the absorber mass is often difficult to adjust, the stiffness in the spring must be the variable component.

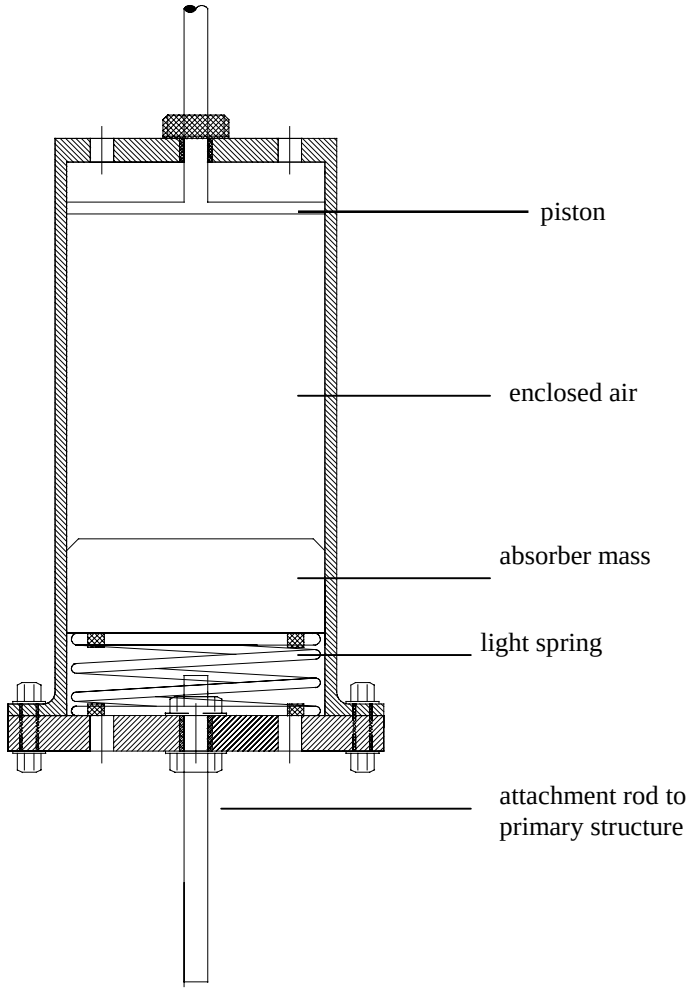

Figure 2.1 - Dynamic Vibration Absorber using enclosed air as a spring variable

Referring to figure 2.1, the absorber consists of a cylindrical shell which contains an absorbing mass. This mass is supported on a light spring which sets the equilibrium displacement of the mass. Variable stiffness is provided by an adjustable enclosed air volume above the mass. Note that the air volume is *not* pressurised.

The spring provides clearance for the mass to displace in both positive and negative directions along the vertical axis. The piston on the top of the cylinder moves to adjust the air volume; varying this volume will vary the stiffness component of the absorber resonance. This piston can be connected to a linear actuator which will be linked to a feedback control signal. The absorber is fixed onto the primary system using a rod protruding from the bottom of the shell.

To reduce the damping caused by the friction between the moving mass and the internal walls, a lubricant will be used. To prevent the internal mass from jamming inside the cylinder, it is important that the thickness of the mass not be too small; if this thickness is small, then the mass can tip to one side during oscillations and jam. The overall length of the absorber can be made smaller by reducing this thickness and inserting a rod through the mass to keep it in line. However, this will only increase the damping due to friction, thus reducing the overall performance of the absorber. As this is the first prototype, carbon steel will be used to construct the shell and absorber mass. Mass considerations will be taken into account in the second prototype.

For the initial testing of this prototype, it was found that the mass of the shell was excessive. This added considerably to the equivalent mass of the secondary system (the secondary system will be detailed later). Thus, the absorber mass was ineffective in controlling the vibration the secondary system. In the design of the second prototype, the mass of the shell will be an important factor.

2.3 SECOND PROTOTYPE

The second prototype was designed with the aim of reducing the overall weight of the absorber. If the mass of the shell is heavy, then the mass of the absorbing mass will have to be increased to ensure an acceptable tolerance level between ω_{11} and ω_{22}. The shell of the second prototype was built using Perspex. This also allows the user to see inside the device while it is in use. The optimal dimension of the enclosed air volume was determined using the following equation.

$$K = \frac{A^2 P}{V}$$

Where K = stiffness provided by the enclosed air (N/m)

A = cross sectional area of the cylinder (m)

P = pressure inside the enclosed volume (N/m^2)

V = enclosed volume (m^3)

The objective was to control the parameters r (radius of the cylinder (m)), and h (height of the enclosed volume (m)), such that the variation in the stiffness provided by the device is maximum (ie. to maximize the device sensitivity).

Arbitrary values of the radius are first chosen to gain an idea of the overall behavior of the stiffness. These can be shown in figure 2.2.

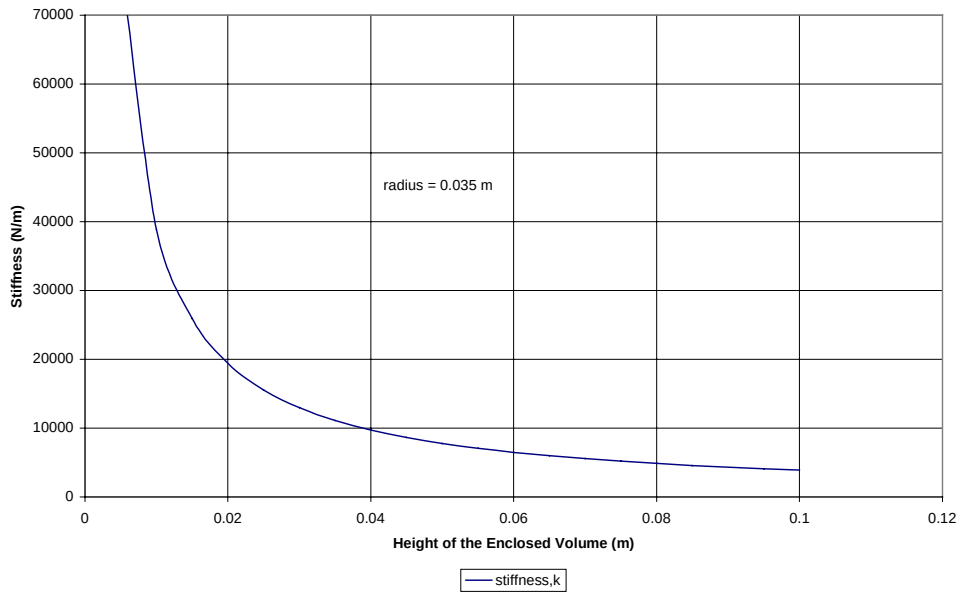

Figure 2.2 – Variation in stiffness when changing the height of the enclosed volume

It can be seen that as the height of the enclosed volume is reduced to 10mm the stiffness increases substantially to 70 kN/m. If the height of the volume is retained at 100mm then the stiffness reduces to 5kN/m. Note that this is only the ideal case where the air is completely sealed in the volume. In practice, the imperfection in the seals and the diaphragm would limit this range in stiffness.

The design of the second prototype is shown in figure 2.3.

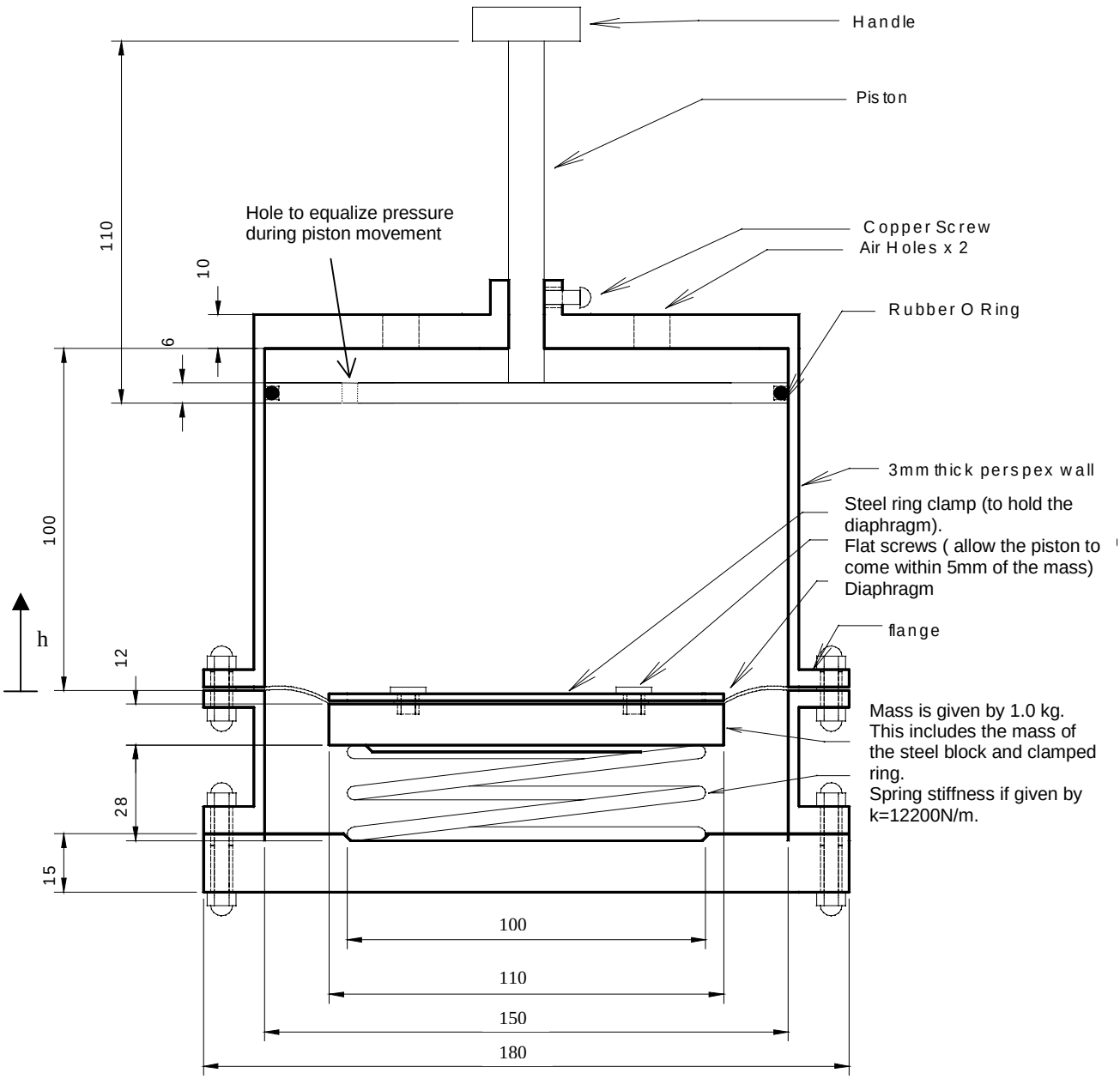

Figure 2.3 – Design of the second prototype

Note that with the second prototype, a rubber diaphragm is used to enclose the volume of air above the absorber mass. If the air is completely sealed from escaping from the space during adjustment of the volume, then the effort required to move the volume-adjusting piston would be excessive. As a result, a single ‘O-ring’ was chosen for the piston seal. With this rather poor seal, the air is still able to escape when the piston is moving up or down, as the rate of this vertical movement is small. While the piston is stationary, the pressure created by the vibrating mass is maintained within the enclosure. It is recognized that this arrangement will place a low-frequency limit on the operation of the device, as the pressure will equalize over time (similar to the equalization of charge in a piezo-electric device placing a low-frequency limit on its operation). The equalization effect is achieved incorporating a hole into the piston (as shown in figure 2.3). However, it is expected that the device will still be able to function in the target span of 30-100 Hz.

2.4 EXPERIMENTAL RESULTS

2.4.1 Frequency Range of Second Prototype

The natural frequency of the absorber is controlled by adjusting the piston vertically at specified distances. The figure below shows the change in natural frequency attainable when the device is attached directly to a shaker. A force transducer is located at the point of attachment, and an accelerometer is located on the absorbing mass, to provide the transfer function.

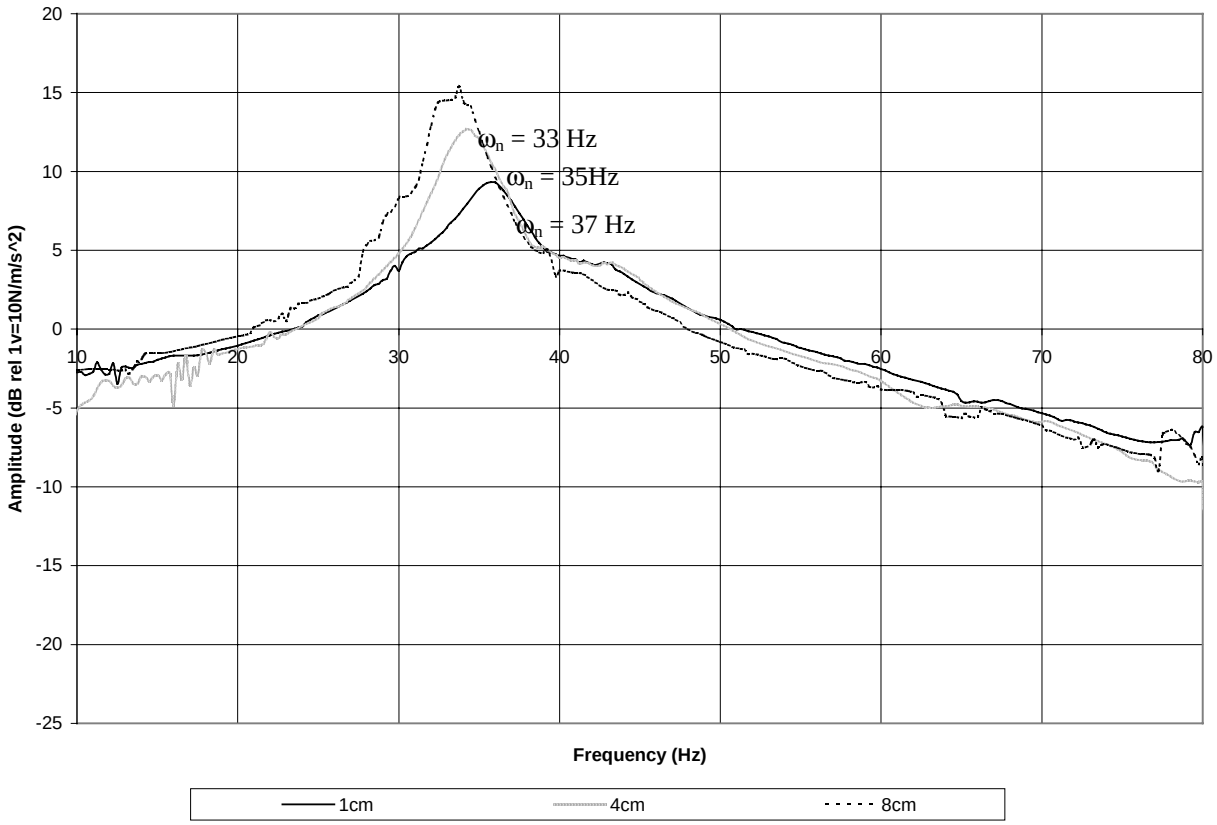

Figure 2.4 – Transfer function of second prototype

Figure 2.4 shows that the natural frequency varies over a range from 33 Hz, when the height of the enclosure is at 8cm, to 37 Hz, when the height is at 1cm. The absorber mass decreases in amplitude by 6 dB as the volume height is decreased from 8cm to 1cm. This is in accordance with the theoretical analysis. As the volume of the enclosure decreases, the amount of "compressible air" becomes less. Hence, with small values the rate of compression per unit displacement of the piston is much greater when the volume is reduced, and so the displacement will also be reduced.

2.4.2 Identified Problems with the Second Prototype

The range in natural frequencies obtained with the absorber device was less than that predicted in the numerical analysis. This is likely due to a number of factors. First, the enclosed air volume was assumed to be ideal, such that the air was neither escaping nor entering into the enclosure while the mass is oscillating. In practise, imperfections in the rubber 'o-ring' and the difficulties in cutting the Perspex to a perfect circle will allow for some air to move between the enclosed volume and the external environment. This will reduce the maximum pressure attainable when the air is compressed by the moving absorber mass, thus reducing the span of natural frequency when the piston is in different positions.

Second, the diaphragm which supports the absorber mass may not be completely uniform after the manufacturing process. The diaphragm used in the device was initially a flat piece of rubber which was heat treated and curved into a membrane. Because of this, the mass which sits on top may still oscillate eccentrically, possessing a moment about the z-axis. This can be illustrated in figure 2.5.

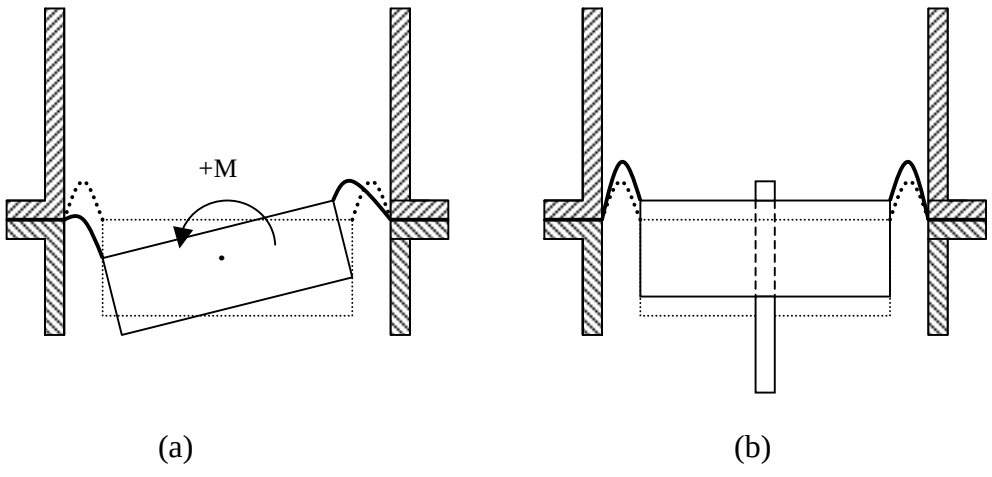

Figure 2.5 Identified problem with absorber mass

This problem could be minimised by manufacturing a rubber membrane via a mould, but this would increase the cost of the device substantially. The alternative was to construct a sliding rod through the absorber mass, so that the mass would move axially along the y-axis without rotation (figure b). However without constant lubrication, the frictional damping between the rod and the mass would affect the performance of the absorber at resonance. Figure 1.2 shows the decrease in attenuation obtainable when there is excessive damping present in the absorber.

A third possibility is that the rubber diaphragm will actually distort under the pressure of the compressed air volume, and so effectively place an upper limit on the compression reached.

2.4.3 Comparison of Experimental with Theoretical Values

The graph below shows the comparison of the experimental values for the stiffness of the absorber with the theoretical values. The values shown are for the enclosed air volume, and does not include the stiffness value provided by the supporting spring (k_{spring} = 12200 N/m).

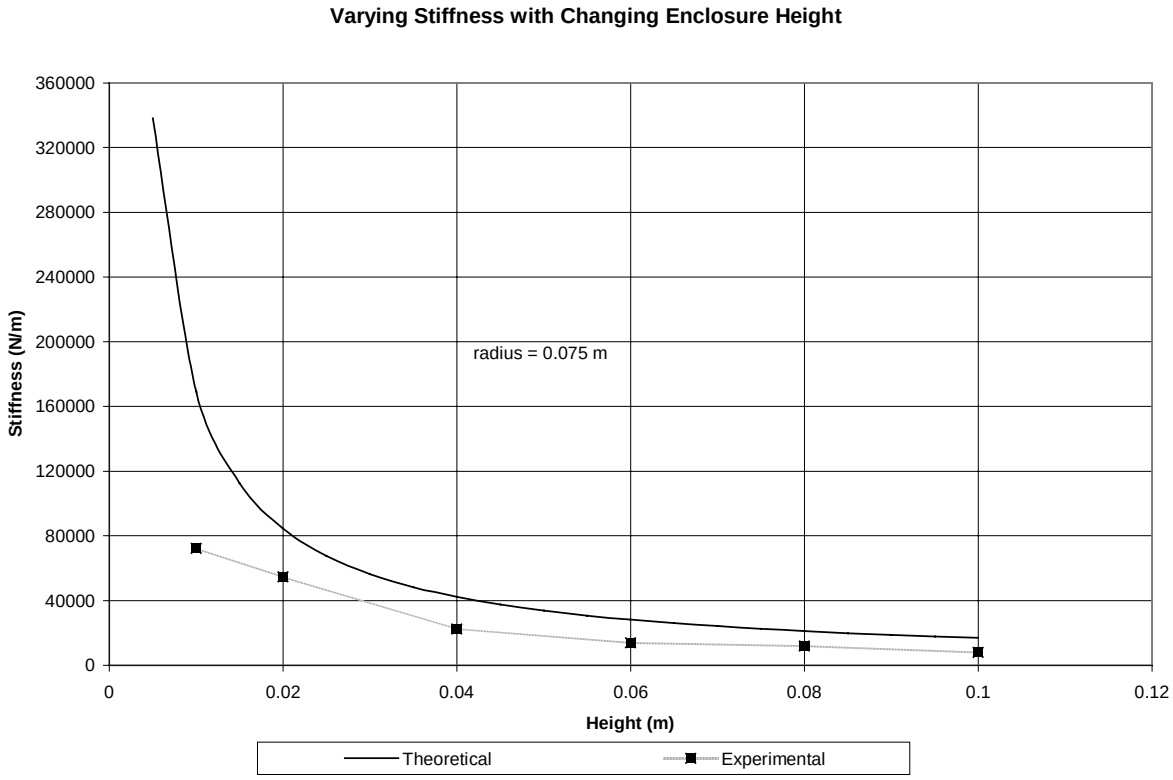

Figure 2.6 Comparison of experimental and theoretical stiffness values

Figure 2.6 shows that the experimental data corresponds to the theoretical values at piston heights above 6cm. When the piston is below this distance, the theoretical values increase at a rate faster than the experimental. This is most likely because the absorber is unable to hold the pressure.

The theoretical stiffness (N/m) value is given by,

$k = \omega_{nt}^2 . m_{eq}$ where m_{eq} (kg) = absorber mass (+ mass of diaphragm and steel cap) + spring mass / 3.

ω_{nt} (rad/s) = the theoretical natural frequency calculated for an ideal case.

And the experimental stiffness value is given by,

$k = \omega_{ne}^2 . m_{eq}$ where ω_{ne} (rad/s) = the experimental natural frequency

$$= \frac{\omega_d}{\sqrt{1-\zeta^2}}$$

ω_d (rad/s) = damped natural frequency

ξ = damping coefficient measured from transfer function.

2.4.4 Identified Problems with Prototype Using Rubber Diaphragm

The damping introduced by the diaphragm was found to be excessive; $\varsigma \approx 0.7$. This would result in the absorber mass oscillating in phase with the primary mass. For a tuned and damped absorber, the reaction force is ideally 90° out of phase with the displacement and the acceleration at the point of interface. Damping could be decreased by reducing the thickness of the diaphragm. However, this will limit the maximum attainable pressure of the enclosed air, as a thin diaphragm will bulge under air pressure.

Performance of the absorber is sensitive to mounting, as the absorber mass is prone to rotational motion as well as displacement. The first attempt of mounting the absorber such that the mass was oscillating horizontally resulted in a frequency function producing two peaks. The second of which could be attributed to the moment action on the mass. The alternative method of mounting the absorber such that the motion was vertical, eliminated the two peaks.

In order to provide a seal for the enclosed air, the piston acting on the enclosed volume has a rubber o-ring around the edges of the piston. Without any form of lubrication, this created excessive friction while moving the position of the piston. This point must be taken when designing the control system for the piston. The motor used to drive the piston must have sufficient power to overcome this friction, if lubrication is not to be used. It was anticipated that the absorber device would be free of maintenance.

There exists a lack of pressure due to distortion of the rubber diaphragm. A thicker diaphragm would reduce the distortion of the diaphragm when it is under air pressure.

2.5 INCORPORATING THE USE OF AN ALUMINIUM DIAPHRAGM

Figure 2.4 showed that the span of the natural frequency of the original absorber air volume was between 33 Hz and 37 Hz. It was necessary to increase this range of frequencies for the absorber to be of practical use. A sheet of aluminium curved into a membrane (as shown in Figure C-2) was trialed as an alternative material to rubber for the diaphragm. The thickness of the aluminium was 0.5 mm. The operating frequencies of the absorber are increased to a greater span. This is illustrated in figure 2.7.

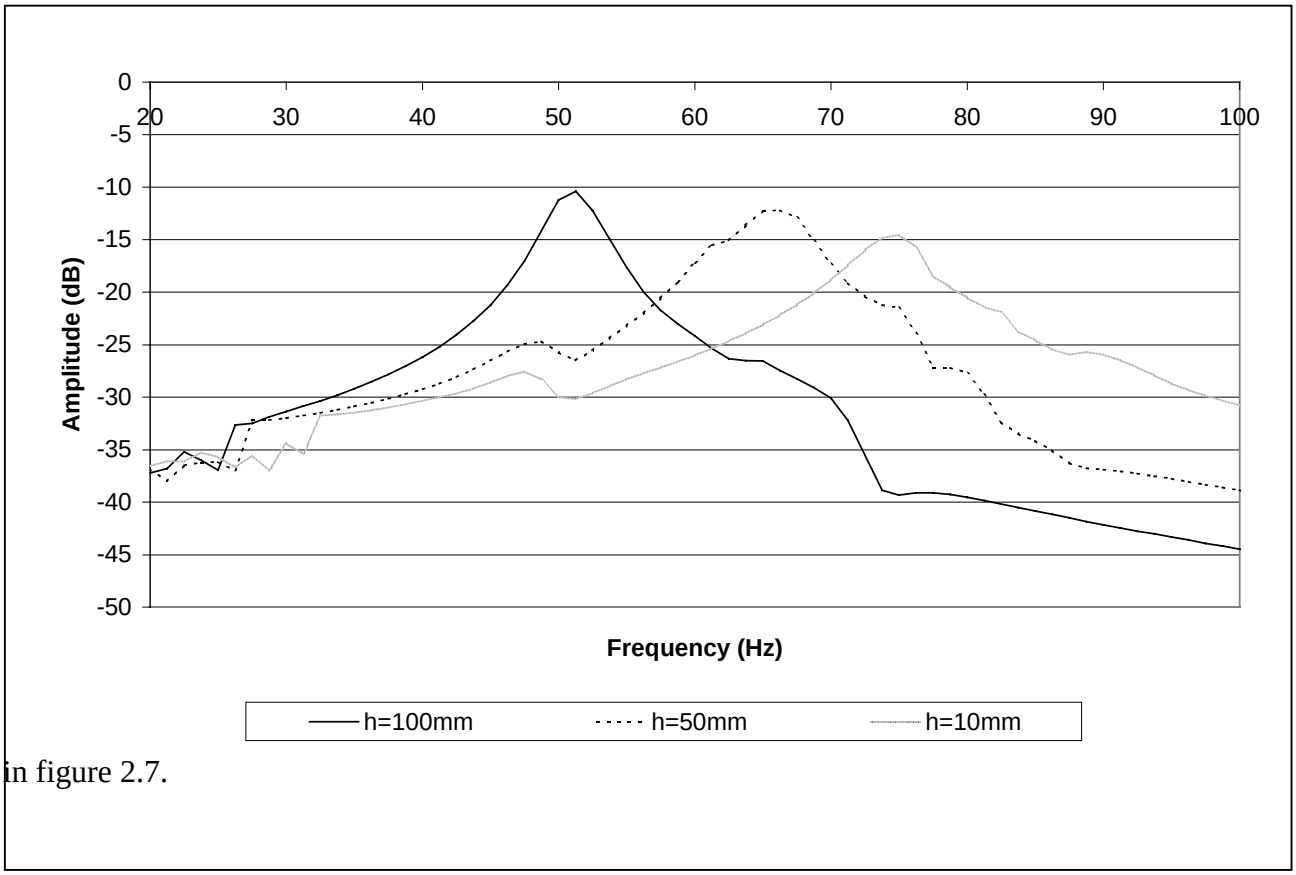

Referring to figure 2.7, it can be surmised that use of the aluminium diaphragm in place of the rubber diaphragm significantly improves the variable stiffness of the device. At a piston height of 100mm, the lowest natural frequency recorded from the transfer function plot was approximately 51 Hz. This compares favourably with the previous value of 33 Hz when the rubber diaphragm was

used. The maximum natural frequency obtained using the aluminium diaphragm was at 75 Hz, with the piston at a height of 10mm. Heights below this value were impractical as the maximum displacement of the mass was 8mm. The workable span of the absorber when using the aluminium increased from 4 Hz to approximately 24 Hz, greatly improving the usability of the device. Note that larger spans would be possible by maintaining a constant pressure above atmospheric. However, this would increase the running cost of the absorber as pressure valves and an intake of airflow would have to be incorporated into the design. Construction costs would also increase as better quality seals would be required to ensure that the increased pressure is maintained.

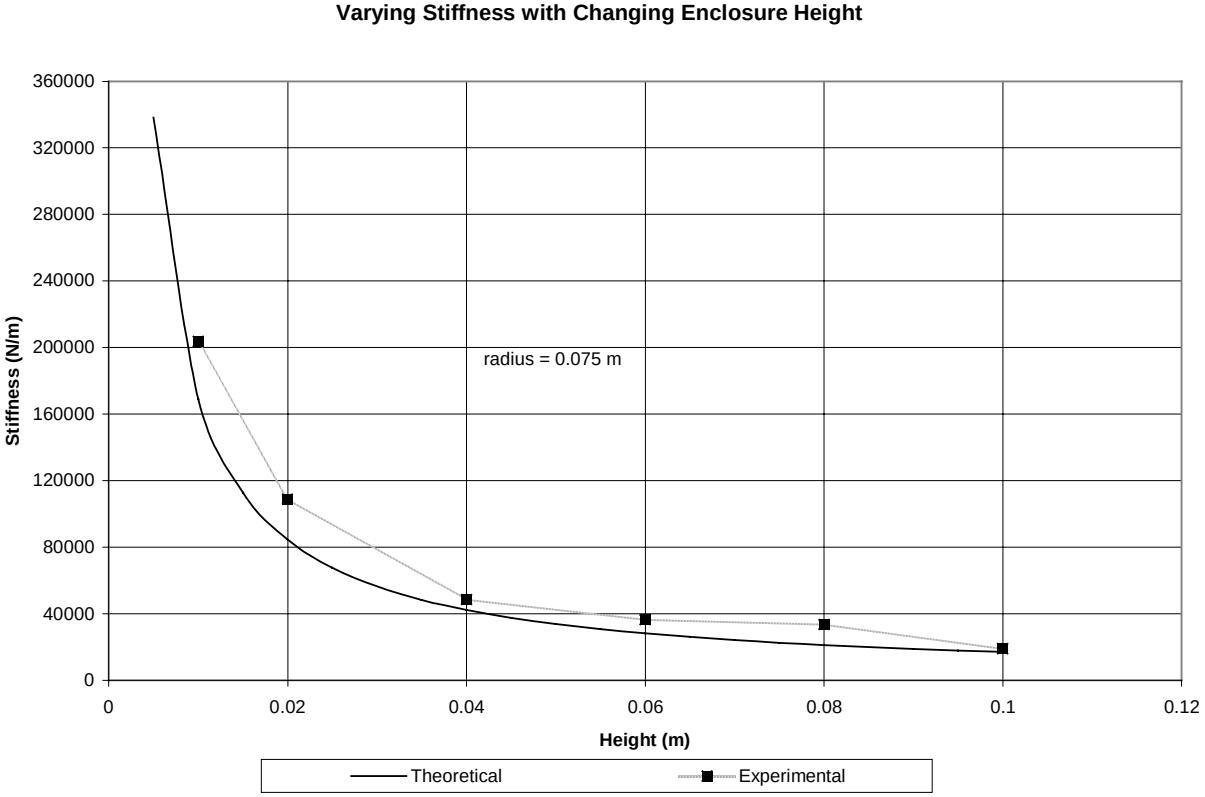

Figure 2.8 – Variation between experimental and theoretical stiffness values for Aluminium diaphragm

Figure 2.8 shows the increase in stiffness achieved when the rubber diaphragm is replaced by an aluminium diaphragm. The range of stiffness is increased from the previous case, and the maximum

stiffness value obtained is greater, when the height of the piston is at 0.01m.

The values obtained for the aluminium diaphragm are slightly higher than the predicted theoretical values, due to the aluminium providing some of the stiffness, in addition to the supporting spring.

2.6 IMPEDANCE OF THE ABSORBER

The peak absorber impedance is given by the equation:

$$H_a\big|_{\max} = m_a.Q_a.\omega_a$$

Where H_a ($N/m^2/s$) = maximum impedance of the absorber.
m_a (kg) = absorber mass.
Q_a = quality factor.
ω_a (rad/s) = natural frequency of absorber.

The quality factor is measured from the transfer function for the aluminium diaphragm graph. The quality factor is a measure of the damping within the system and is represented by the sharpness of the peak (3dB bandwidth) at the point of resonance.

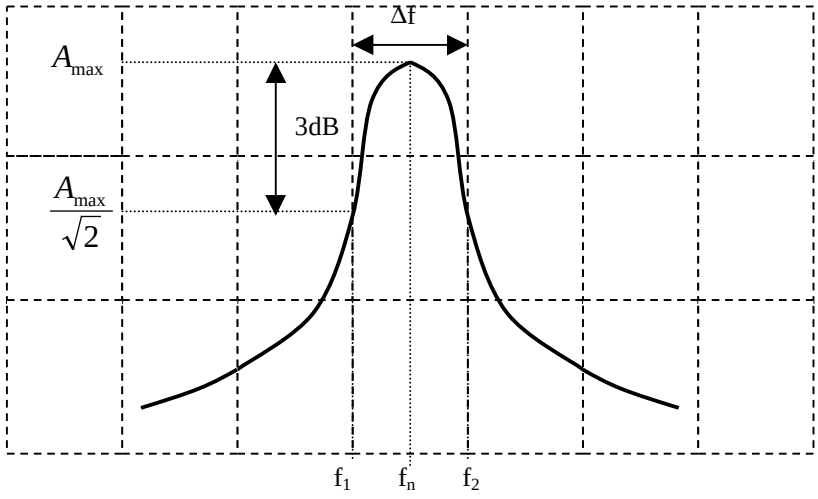

Figure 2.9 Harmonic response curve showing bandwidth and half power points

From figure 2.7, at a resonance of 51.25 Hz,

$$Q\big|_{3dB} = \frac{f}{\Delta f}$$
$$= \frac{51.25}{53.75 - 48.75}$$
$$= 10.25$$

For m = 1.125kg, $\omega_a = 51.25 \times 2\pi$

$$H_a\big|_{\max} = 1.125 \times 10.25 \times 322.0$$

$$= 3713 N/m \ \ /s$$

The impedance of the absorber exceeds that of the primary structure. This is a requirement if the absorber device is to be effective. At resonance, when the absorber device has an impedance exceeding that of the primary structure, the ratio of the motion of the primary structure before and after absorber installation can be shown to be (Von Flotow, 1994),

$$\left.\frac{u_b}{u_F}\right|_{\omega_a} = \frac{H_b(\omega_a)}{H_a\big|_{\max}}$$

$$= \frac{H_b(\omega_a)}{m_a Q_a \omega_a}$$

2.7 PERFORMANCE OF THE ABSORBER

To test the performance of the absorber, it was mounted onto a simply supported vibrating beam. This test rig is also used for the testing of the Dual Cantilevered Mass Absorber, and will be discussed in detail in section 3.5.4. The absorber was clamped onto the beam, and a shaker is attached at a point along the beam to excite it, as shown in figure 2.10. The aluminium diaphragm dynamic absorber was then manually tuned until its natural frequency coincides with the resonance frequency of the beam. A transfer function is then taken between the point of attachment of the absorber and the point near the excitation force.

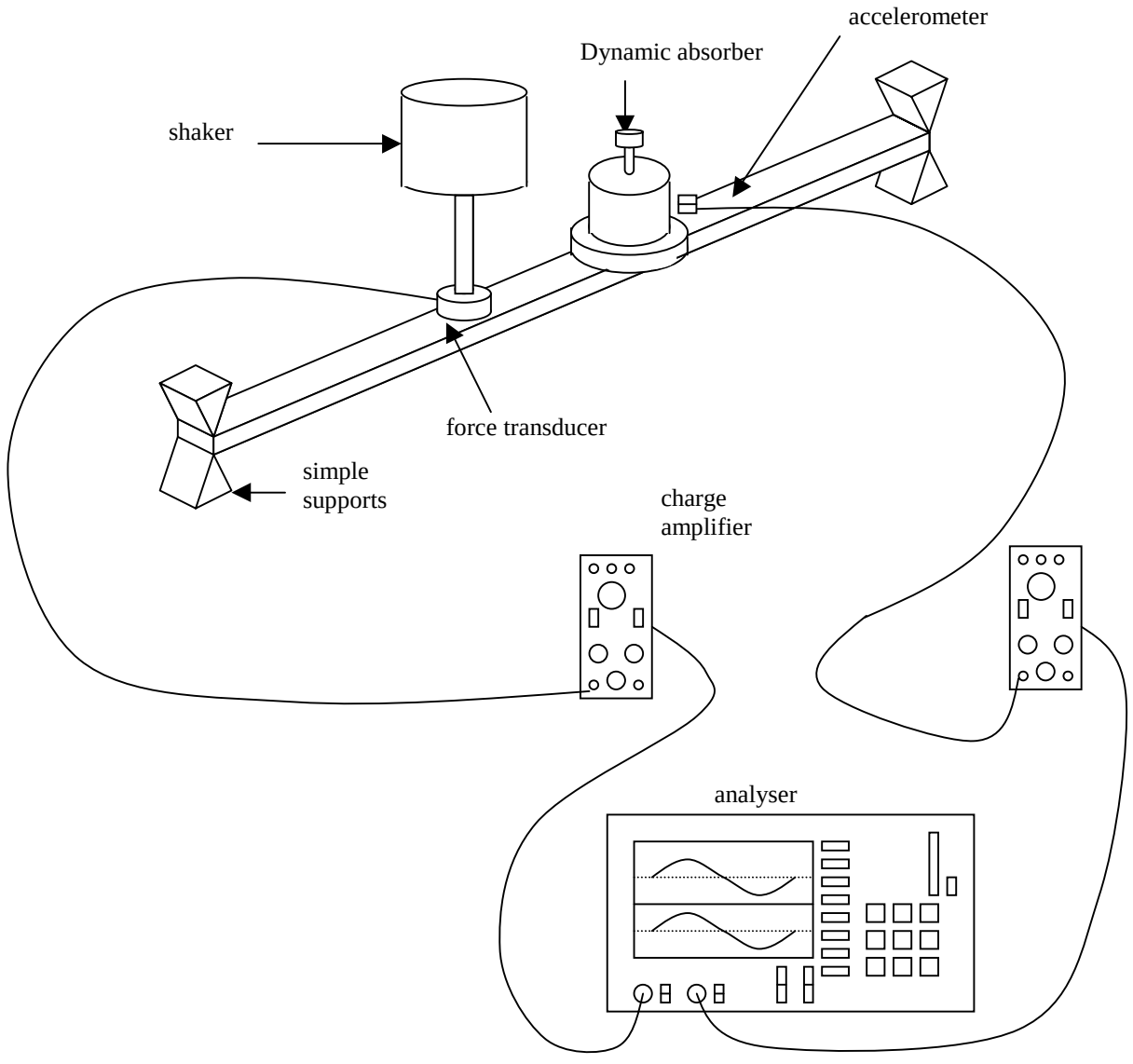

Figure 2.10 - Experimental Setup for Aluminium Absorber

The frequency response obtained from the experiment is shown in figure 2.11

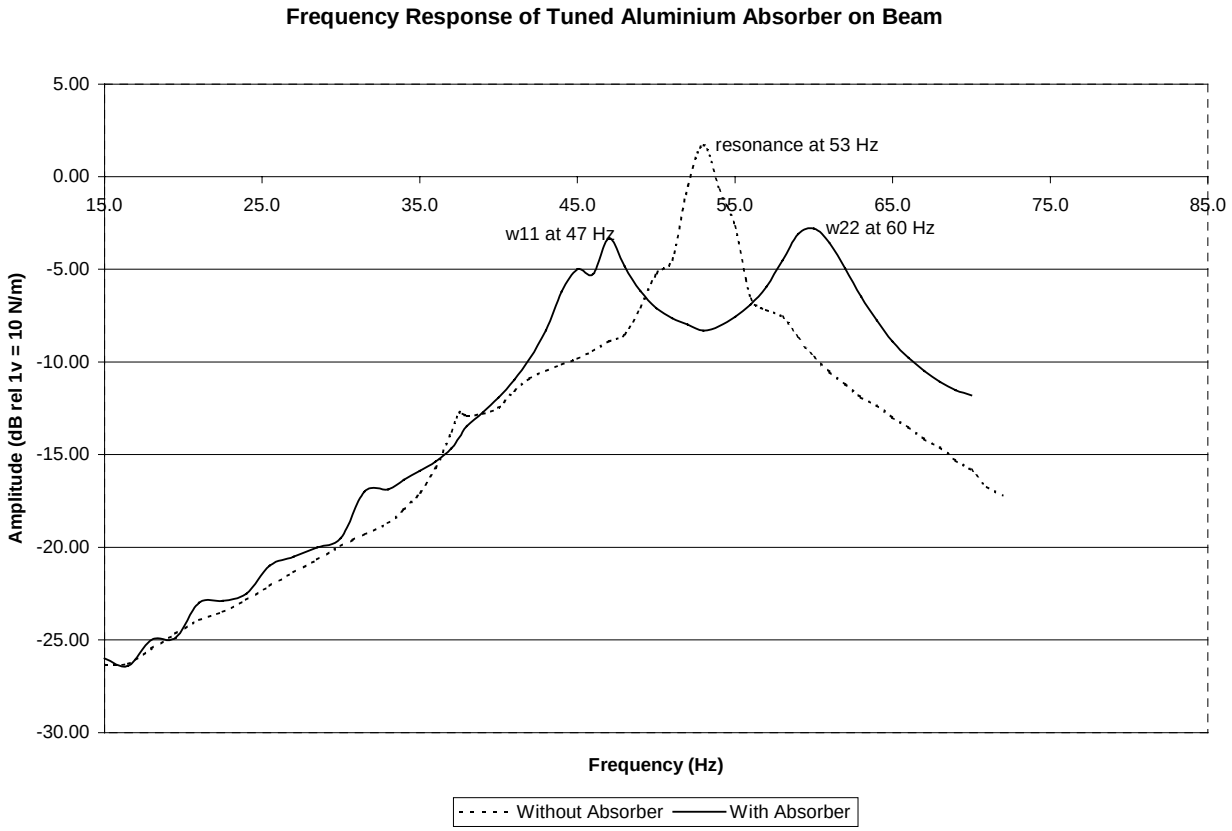

Figure 2.11 Frequency response of Aluminium Diaphragm Dynamic Vibration Absorber

The frequency response on the beam shows that when the absorber is tuned to the resonance frequency of 53 Hz, there is an attenuation of 10 dB. This level of attenuation can be further increased if the damping within the absorber is reduced. The two peaks produced (ω_{11} and ω_{22}) are at 47 Hz and 60 Hz respectively.

2.8 SUMMARY

In this chapter, two prototypes for dynamic vibration absorbers have been designed, using air as a spring variable. The range in stiffness achievable using this mechanism has been investigated and appropriate dimensions have been chosen for the design of the second absorber. The testing of the absorber has been undertaken and further problems have been identified and addressed:

1. The operating frequency range (which made the absorber impractical when using the rubber diaphragm) has been improved by using the aluminium diaphragm incorporated into the design. The bulging effect on the rubber diaphragm has been minimized with the aluminium diaphragm, thus the maximum attainable pressure within the enclosed volume has been increased.
2. The overall mass of the absorber has been reduced, by construction of the second prototype from Perspex. This has reduced the equivalent mass required for the absorbing mass to control the vibration.

The absorber has been shown to be effective in obtaining a small reduction in the vibration of the test rig, when correctly tuned.

CHAPTER 3 DUAL CANTILEVERED MASS DYNAMIC VIBRATION ABSORBER

3.1 INTRODUCTION

Studies directed at assessing the effectiveness and practicality of the first absorber, which used air as a variable spring, indicated two major problems with the design:

1. A limitation in the range of frequencies over which the device could be used, imposed by material limitations (particularly in the case of the rubber diaphragm, which bulged under pressure)
2. A high level of damping inherent in the arrangement

As such, a second improved absorber design will be investigated. Torsional vibration absorbers have been used for many applications, such as reduction of vibration in aircraft fuselages. An adaptation of this idea will be treated as a replacement for the initial prototype. Referring to figure 3.1, a cantilevered mass arrangement consisting of two masses (the absorber mass) linked by a beam which is fixed at the centre will be used here as the absorber. The fixed centre is attached directly to the vibrating surface.

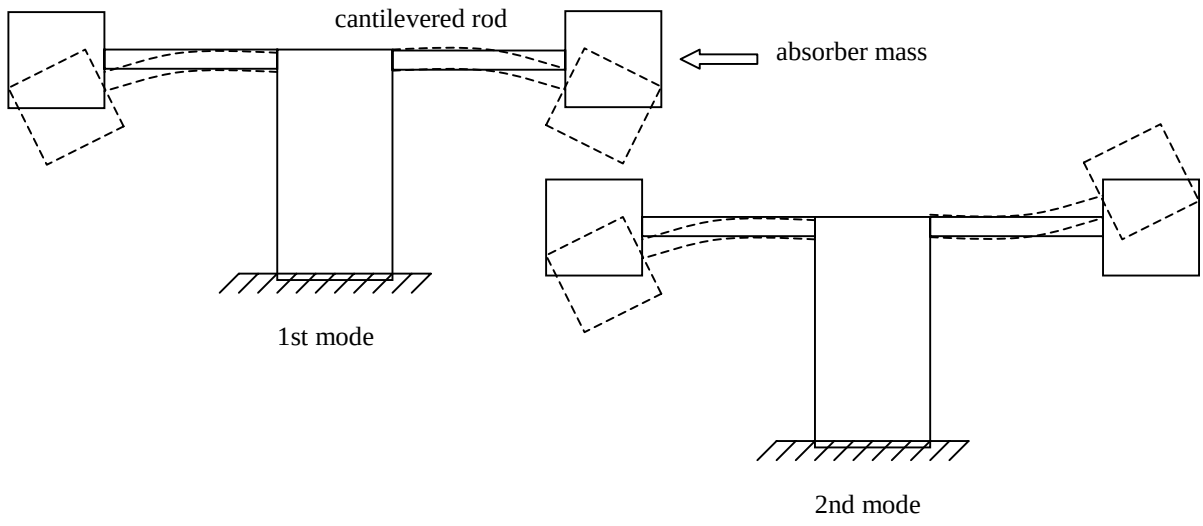

Figure 3.1 – The first 2 modes of the cantilevered absorber

The effective motion of the each mass is that of a cantilever. It is possible to tune the absorber using some adaptive strategy, by moving the masses along the beams. This results in a change in natural frequency of the device and thus a change in the notch (absorbed) frequency. Theoretical analysis of the cantilevered absorber can be undertaken using the impedance method (Plunket, 1958). The motion of a structure can be characterised by its impedance, expressed as the ratio of an exciting force at a particular frequency to the resulting velocity at another point on the structure at the same frequency. Once the impedance of a structure is known, prediction of the motion of the structure due to other forcing functions is possible.

It is possible (and possibly more accurate) to design this absorber using finite element analysis, undertaken here using the computer package Ansys. With this, the resonance frequencies of the first 5 modes can be found. The Ansys program is included in appendix A. Later, the absorber is to be attached to a uniform beam undergoing transverse vibration. The design of the test rig is discussed in section 3.5.4. The aim is to minimise the local vibration at a sensor location on the beam.

3.2 INITIAL THEORETICAL ANALYSIS OF CANTILEVERED ABSORBER USING DISCRETE SYSTEM METHOD

As a simplified first analysis, the absorber system is assumed to be composed of discrete systems. The absorber mass at the end of the rod is assumed to be one system, and the rod itself is another. If the damping present in the system is neglected, Dunkerleys equation can be used for analysis. Dunkerleys equation states that for a multi degree-of-freedom system, the inverse of the fundamental frequency (Seto, 1964),

$$\frac{1}{\omega_1^{\,2}} = \frac{1}{\omega_{11}^{\,2}} + \frac{1}{\omega_{22}^{\,2}} + ... + \frac{1}{\omega_{nn}^{\,2}} = \sum_{i=1}^{n} \frac{1}{\omega_{ii}^{\,2}}$$

where $\omega_{11}, \omega_{22} \ldots \omega_{nn}$ are the corresponding natural frequencies of each component of the system acting alone

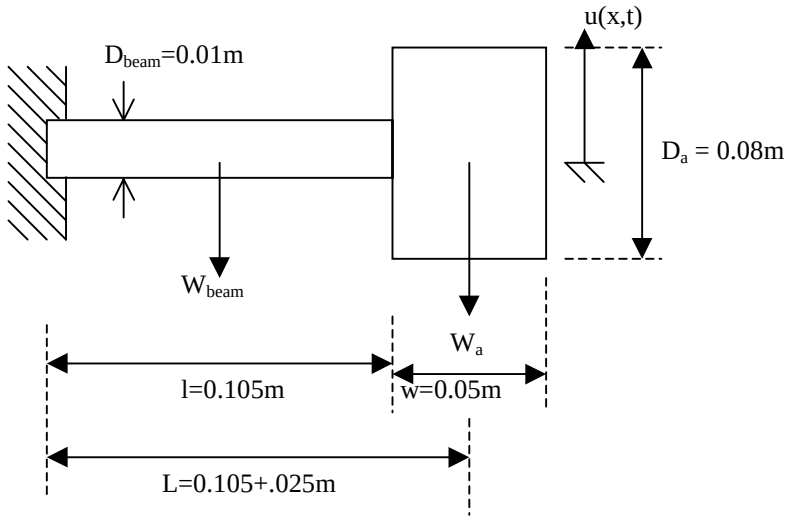

Figure 3.3 – Dimensions used for Discrete System Analysis

For the natural frequency, ω_b of a cantilevered beam of mass, m_1,

$$\omega_b^{\,2} = 12.7.\frac{EI}{m_1 l^3}$$

For the absorber device, two rods are in parallel, with the mass attached at x=L.

As $k = \omega^2 m$,

$$k = 12.7\frac{EI}{l^3}$$

The total stiffness produced by the 2 rods in parallel is,

$k_t = k_1 + k_2$

$$k = 12.7\frac{EI}{l^3} \times 2$$
$$= 25.4\frac{EI}{l^3}$$
$$\therefore \omega_b{}^2 = 25.4\frac{EI}{ml^3}$$

For the natural frequency, ω_a of a cantilevered beam of negligible mass with a concentrated mass attached at one end,

$$\omega_a{}^2 = \frac{3EI}{ml^3}$$

Using Dunkerleys equation,

$$\frac{1}{\omega_1{}^2} = \frac{1}{\omega_b{}^2} + \frac{1}{\omega_a{}^2}$$
$$= \frac{m_b l^3}{25.4EI} + \frac{m_a l^3}{3EI}$$
$$= \frac{3m_b l^3 + 25.4m_a l^3}{76.2EI}$$
$$\therefore \omega_1{}^2 = \frac{76.2EI}{3m_b l^3 + 25.4m_a l^3}$$

$$\therefore \omega = \sqrt{\frac{76.2EI}{3m_b l^3 + 25.4m_a l^3}}$$

For the material properties of steel,

E = 207 GPa, (Modulus of Elasticity)

$I = \pi R^4/4 = \pi(0.005)^4/4 = 4.91\times 10^{-10}\ m^4$. (Second Moment of Area)

$\rho = 7800\ kg/m^3$. (density)

$m_b = \pi(0.005)^2.(0.105).(7800).2$

$= 0.129\ kg$

$m_a = \pi(0.04)^2.(0.05).7800$

$= 1.96\ kg$

$L = 0.105 + 0.025$

$= 0.13m$

$$\therefore \omega_1 = \sqrt{\frac{76.2\times 207\times 10^9 \times 4.91\times 10^{-10}}{3\times 0.129\times 0.13^3 + 25.4\times 1.96\times 0.13^3}}$$

$$= 265.0 rad/s$$
$$= 42.2 Hz$$

This value is lower than the value obtained for the experiment (46.25 Hz) at L=0.105m, which is common for such analysis.

3.3 THEORETICAL ANALYSIS OF THE CANTILEVERED ABSORBER USING CONTINUOUS SYSTEM THEORY

To improve upon the previous "simple" analysis, the following is a derivation to calculate the natural frequencies of the dual cantilevered mass device. The device is first assumed to be symmetric about the centre line y-axis, and modelled as a cantilevered cylindrical beam with a uniform mass attached to the end.

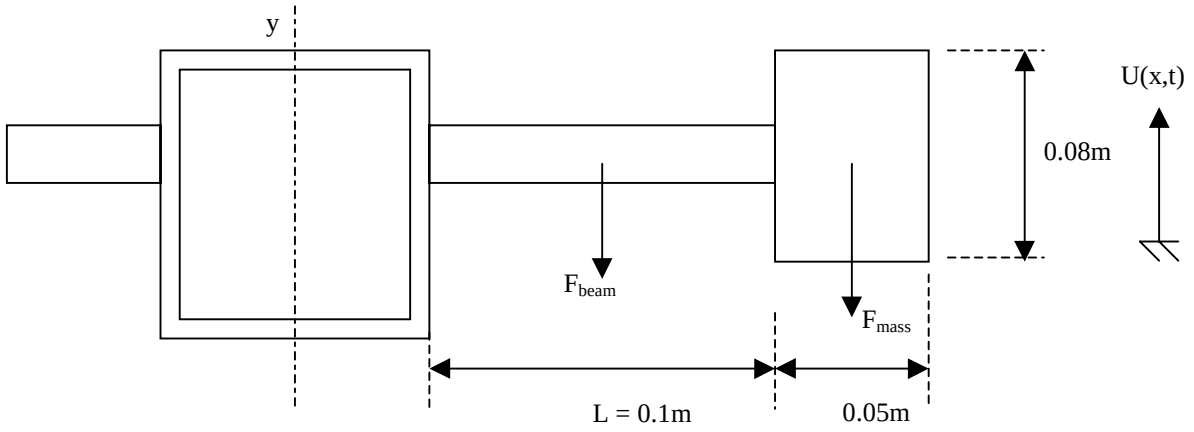

Figure 3.4 – Dimensions used for continuous system analysis

Firstly, the frequency equation is found using the method of separation of variables (Tse *et. al*.) The longitudinal displacement of the mass is assumed to be of the form,

$$u(x,t) = \phi(x).q(t) \qquad \textbf{(3-1)}$$

where $\phi(x)$ is a function involving only x, and q(t) is a function involving only time, t.

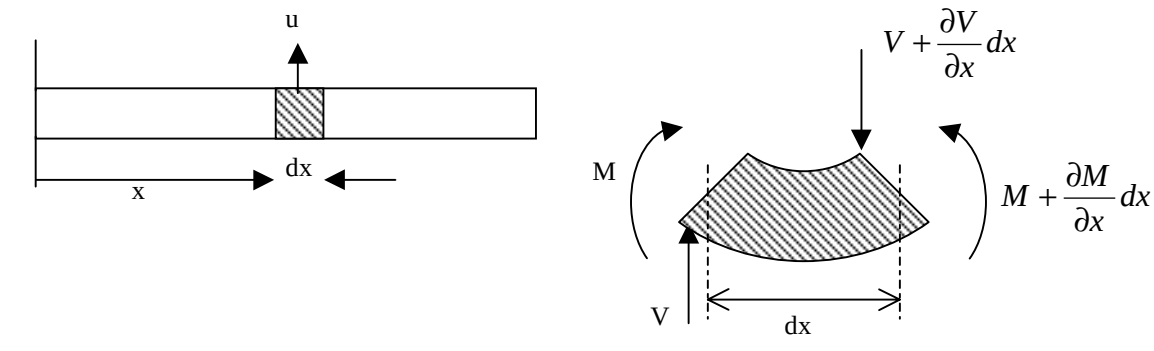

Figure 3.5 – Shear and moment sign conventions

Applying Newton's laws in the lateral direction gives (Mc Callion, 1973),

$$-V + V + \frac{\partial V}{\partial x}dx = m.dx.\frac{\partial^2 u}{\partial t^2}$$

$$\therefore m\frac{\partial^2 u}{\partial t^2}dx = -(V + \frac{\partial V}{\partial x}dx) + V$$

For m= ρA= mass/unit length (kg/m).
where ρ = density (kg/m^3)
and A = cross sectional area of beam (kg^3)

$$\therefore m\frac{\partial^2 u}{\partial t^2} = \frac{\partial V}{\partial x} \quad \textbf{(3-2)}$$

Taking the moment about a point on the right side of the element,

$$+\circlearrowleft \sum M_{right\_side} = 0$$

$$\therefore -M + M + \frac{\partial M}{\partial x}dx - Vdx = 0$$

$$\therefore V = -\frac{\partial M}{\partial x}$$

Using this result in Equation (3-2) gives,

$$\frac{\partial^2 M}{\partial x^2} + m\frac{\partial^2 u}{\partial t^2} = 0$$

Using the Bernoulli-Euler beam theory, the applied moment is related to the radius of curvature by,

$$EI\frac{\partial^2 u}{\partial x^2} = M, \quad \textbf{(3-3)}$$

Combining Equation (3-2) and Equation (3-3) forms the beam equation for lateral vibration,

$$m\frac{\partial^2 u}{\partial t^2} = -\frac{\partial^2}{\partial x^2}\left(EI\frac{\partial^2 u}{\partial x^2}\right)$$

$$= \frac{\partial^2 u}{\partial t^2} + \frac{EI}{m}.\frac{\partial^4 u}{\partial x^4} = 0 \quad \textbf{(3-4)}$$

This is the equation of motion for the element, dx.

If the wave equation, (3-1) is substituted into Equation (3-4), this gives

$$\phi \frac{d^2q}{dt^2} + \frac{EI}{m} q \frac{d^4\phi}{dx^4} = 0 \qquad As \frac{\partial^4 u}{\partial x^4} = q \frac{\partial^4 \phi}{\partial x^4} and \frac{\partial^2 u}{\partial t^2} = \phi \frac{\partial^2 q}{\partial t^2}$$

$$\therefore -\frac{EI}{m} \cdot \frac{1}{\phi} \cdot \frac{d^4\phi}{dx^4} = \frac{1}{q} \cdot \frac{d^2q}{dt^2} \qquad \textbf{(3-5)}$$

As the right hand side of Equation (3-5) is independent of x, and the left hand side is independent of t, then they must both equal a constant, as the equation is true for all values of x and t.

So let,

$$-\frac{EI}{m} \cdot \frac{1}{\phi} \cdot \frac{d^4\phi}{dx^4} = -w^2$$

$$\therefore \frac{d^4\phi}{dx^4} - \frac{m\omega^2}{EI}\phi = 0 \qquad \textbf{(3-6)}$$

where ω^2 is a constant

Similarly, as

$$\frac{1}{q} \cdot \frac{d^2q}{dt^2} = -\omega^2$$

$$\therefore \frac{d^2q}{dt^2} + \omega^2 q = 0 \qquad \textbf{(3-7)}$$

Equations (3-6) and (3-7) form two linear differential equations. The solution of each of these can be shown to be,

$$\phi(x) = C_1 \sin \beta x + C_2 \cos \beta x + C_3 \sinh \beta x + C_4 \cosh \beta x \quad \textbf{(3-8)}$$

and

$$q(t) = C_5 \sin \omega t + C_6 \cos \omega t \quad \textbf{(3-9)}$$

So using Equation (3-1),

$$\boxed{u(x,t) = (C_1 \sin \beta x + C_2 \cos \beta x + C_3 \sinh \beta x + C_4 \cosh \beta x)(C_5 \sin \omega t + C_6 \cos \omega t)} \quad \textbf{(3-10)}$$

$$\textit{by letting} \quad \beta^4 = \frac{m\omega^2}{EI}$$

This is the general solution to a beam undergoing lateral vibration. To find the frequency equation for the cantilevered absorber mass attached to the end of the cylindrical uniform beam, the boundary conditions must be known. For the purpose of this study, the beam is assumed to be rigidly clamped to the wall of the aluminium block. (Thus u(x,t)=0). The boundary conditions, however, are normally difficult to implement exactly in practical applications. Common boundary conditions for lateral vibration in beams are shown in figure 3.6 (Tse *et al*,1978).

Left Boundary Conditions | Beam End Conditions | Right Boundary Conditions

u(0,t)=0 $\quad \frac{\partial u}{\partial x} = 0$ 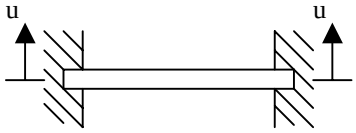 u(l,t)=0 $\quad \frac{\partial u}{\partial x} = 0$

Fixed

$EI\frac{\partial^2 u}{\partial x^2} = 0$ $\quad EI\frac{\partial^3 u}{\partial x^3} = 0$ 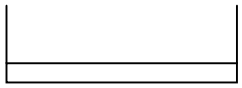 $EI\frac{\partial^2 u}{\partial x^2} = 0$ $\quad EI\frac{\partial^3 u}{\partial x^3} = 0$

Free

u(0,t)=0 $\quad EI\frac{\partial^2 u}{\partial x^2} = 0$ 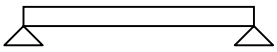 u(0,t)=0 $\quad EI\frac{\partial^2 u}{\partial x^2} = 0$

Simply Supported

$EI\frac{\partial^2 u}{\partial x^2} = k_t\frac{\partial u}{\partial x}$ $\quad EI\frac{\partial^3 u}{\partial x^3} = -k_t u$ 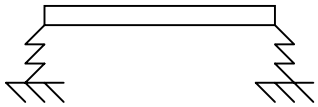 $EI\frac{\partial^2 u}{\partial x^2} = -k_t\frac{\partial u}{\partial x}$ $\quad EI\frac{\partial^3 u}{\partial x^3} = k_t u$

Spring Load

$EI\frac{\partial^2 u}{\partial x^2} = 0$ $\quad EI\frac{\partial^3 u}{\partial x^3} = -m\frac{\partial^2 u}{\partial t^2}$ 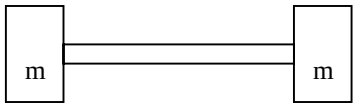 $EI\frac{\partial^2 u}{\partial x^2} = 0$ $\quad EI\frac{\partial^3 u}{\partial x^3} = m\frac{\partial^2 u}{\partial t^2}$

Inertia Load

$\frac{\partial u}{\partial x} = slope\_component$ $\quad \frac{\partial^2 u}{\partial x^2} = moment\_component$ $\quad \frac{\partial^3 u}{\partial x^3} = shear\_component$

Figure 3.6 Boundary conditions for lateral vibration in a beam

So for a beam which has a clamped end on the left, and an inertia load on the right hand side, the following boundary conditions apply.

At the fixed end (x=0), the slope and deflection are zero,

$$u(0,t) = 0 \tag{3-11}$$

$$\frac{\partial u(0,t)}{\partial x} = 0 \tag{3-12}$$

At the mass loaded end (x=l), the moment is zero,

$$M = 0 \qquad or \qquad EI\frac{\partial^2 u}{\partial x^2} = 0 \tag{3-13}$$

And the shear force at this end is equivalent to the force × acceleration of the mass,

$$V = m\frac{\partial^2 u}{\partial t^2} \qquad or \qquad EI\frac{\partial^3 u}{\partial x^3} = m\frac{\partial^2 u}{\partial t^2} \tag{3-14}$$

Using the first boundary condition, and using Equation (3-11) in (3-8),

$$x(0,t) = 0,$$

$$\therefore \quad \phi(0) = C_2 \cos\beta(0) + C_4 \cosh\beta(0) = 0$$

$$\therefore \qquad as \qquad \cos(0) \quad and \quad \cosh(0) \neq 0$$

$$\therefore \quad C_2 + C_4 = 0 \tag{3-15a}$$

Using the second boundary condition, Equation (3-12),

$$As \quad \frac{\partial u(x)}{\partial x} = \beta(C_1 \cos\beta x - C_2 \sin\beta x + C_3 \cosh\beta x + C_4 \sinh\beta x)$$

$$then \quad \frac{\partial u(0,t)}{\partial x} = \beta(C_1 \cos\beta(0) + C_3 \cosh\beta(0)) = 0$$

$$\therefore \quad C_1 + C_3 = 0 \tag{3-15b}$$

Thus, using Equations (3-15a) and (3-15b) in (3-8) gives

$$\phi(x) = C_1 \sin \beta x + C_2 \cos \beta x - C_1 \sinh \beta x - C_2 \cosh \beta x$$

$$= C_1(\sin \beta x - \sinh \beta x) + C_2(\cos \beta x - \cosh \beta x) \qquad \textbf{(3-16)}$$

$$\therefore \frac{\partial u(x,t)}{\partial x} = \frac{d\phi}{dx} = \beta\left(C_1 \cos \beta x - C_2 \sin \beta x - C_1 \cosh \beta x - C_2 \sinh \beta x\right)$$

$$= \beta\left(C_1(\cos \beta x - \cosh \beta x) + C_2(-\sin \beta x - \sinh \beta x)\right)$$

$$\textit{and} \quad \frac{\partial^2 u(x,t)}{\partial x^2} = \frac{d^2\phi}{dx^2} = \beta^2\left(-C_1 \sin \beta x - C_2 \cos \beta x - C_1 \sinh \beta x - C_2 \cosh \beta x\right)$$

$$= -\beta^2\left(C_1(\sin \beta x + \sinh \beta x) + C_2(\cos \beta x + \cosh \beta x)\right)$$

$$\textit{and} \quad \frac{\partial^3 u(x,t)}{\partial x^3} = \frac{d^3\phi}{dx^3} = \beta^3\left(-C_1 \cos \beta x + C_2 \sin \beta x - C_1 \cosh \beta x - C_2 \sinh \beta x\right)$$

$$= \beta^3\left(C_1(-\cos \beta x - \cosh \beta x) + C_2(\sin \beta x - \sinh \beta x)\right)$$

Using the third boundary condition, Equation (3-13),

$$-EI\beta^3\left(C_1(\sin \beta x + \sinh \beta x) + C_2(\cos \beta x + \cosh \beta x)\right) = 0$$

$$\therefore \quad \textit{as} \quad EI\beta^3 \neq 0,$$

$$\therefore \quad C_1(\sin \beta x + \sinh \beta x) + C_2(\cos \beta x + \cosh \beta x) = 0 \qquad \textbf{(3-17)}$$

Now we assume that q(t) has the form,

$$q(t) = \sin \omega t$$

$$\therefore \quad u(x,t) = \phi(x) \sin \omega t$$

$$\textit{and} \quad \frac{\partial u(x,t)}{\partial t} = \omega\phi(x) \cos \omega t$$

$$\textit{and} \quad \frac{\partial^2 u(x,t)}{\partial t^2} = -\omega^2\phi(x) \sin \omega t$$

From Equation (3.16),

$$\frac{\partial^2 u(x,t)}{\partial t^2} = -\omega^2 C_1(\sin\beta x - \sinh\beta x) + C_2(\cos\beta x - \cosh\beta x)\sin\omega t \qquad \textbf{(3-18)}$$

Using the fourth boundary condition, Equation (3-14),

$$EI\frac{\partial^3 u(l,t)}{\partial x^3} = m\frac{\partial^2 u(l,t)}{\partial t^3}$$

$$\therefore \quad EI\beta^3\left(-C_1\cos\beta l + C_2\sin\beta l - C_1\cosh\beta l - C_2\sinh\beta l\right)(\sin\omega t)$$

$$= -\omega^2 m\left(C_1\sin\beta l + C_2\cos\beta l - C_1\sinh\beta l - C_2\cosh\beta l\right)(\sin\omega t)$$

$$\therefore \quad EI\beta^3\left(-C_1(\cos\beta l + \cosh\beta l) + C_2(\sin\beta l - C_2\sinh\beta l)\right)$$

$$= -\omega^2 m\left(C_1(\sin\beta l - \sinh\beta l) + C_2(\cos\beta l - \cosh\beta l)\right)$$

from Equation (3.17),

$$C_1 = -C_2\frac{(\cos\beta l + \cosh\beta l)}{(\sin\beta l + \sinh\beta l)}$$

$$\therefore \quad EI\beta^3\left(C_2\frac{(\cos\beta l + \cosh\beta l)}{(\sin\beta l + \sinh\beta l)}(\cos\beta l + \cosh\beta l) + C_2(\sin\beta l - C_2\sinh\beta l)\right)$$

$$= \omega^2 m\left(C_2\frac{(\cos\beta l + \cosh\beta l)}{(\sin\beta l + \sinh\beta l)}(\sin\beta l - \sinh\beta l) - C_2(\cos\beta l - \cosh\beta l)\right)$$

Division by C_2 from both sides gives,

$$EI\beta^3(\cos\beta l + \cosh\beta l)(\cos\beta l + \cosh\beta l) + EI\beta^3(\sin\beta l - \sinh\beta l)(\sin\beta l + \sinh\beta l)$$

$$= \omega^2 m(\cos\beta l + \cosh\beta l)(\sin\beta l - \sinh\beta l) + \omega^2 m(-\cos\beta l + \cosh\beta l)(\sin\beta l + \sinh\beta l)$$

$$\therefore \quad \frac{EI\beta^3}{\omega^2 m}\left[(\cos^2\beta l + 2\cos\beta l\cosh\beta l + \cosh^2\beta l) + (\sin^2\beta l + \sin\beta l\sinh\beta l - \sin\beta l\sinh\beta l - \sinh^2\beta l)\right]$$

$$= \sin\beta l\cos\beta l - \cos\beta l\sinh\beta l + \sin\beta l\cosh\beta l - \sinh\beta l\cosh\beta l$$

$$-\sin\beta l\cos\beta l - \cos\beta l\sinh\beta l + \sin\beta l\cosh\beta l + \sinh\beta l\cosh\beta l$$

$$\therefore \quad \frac{EI\beta^3}{\omega^2 m}\left[(\sin^2 \beta l + \cos^2 \beta l) + 2\cos\beta l \cosh\beta l + (\cosh^2 \beta l - \sinh^2 \beta l)\right]$$

$$= -2\cos\beta l \sinh\beta l + 2\sin\beta l \cosh\beta l$$

$$\therefore \quad \frac{EI\beta^3}{\omega^2 m}\left[1 + 2\cos\beta l \cosh\beta l + 1\right]$$

$$= -2\cos\beta l \sinh\beta l + 2\sin\beta l \cosh\beta l$$

$$\therefore \quad \frac{EI\beta^3}{\omega^2 m}\left[2 + 2\cos\beta l \cosh\beta l\right] + 2\cos\beta l \sinh\beta l - 2\sin\beta l \cosh\beta l = 0$$

$$\therefore \quad EI\beta^3(1 + \cos\beta l \cosh\beta l) + \omega^2 m(\cos\beta l \sinh\beta l - \sin\beta l \cosh\beta l) = 0 \qquad \textbf{(3-19)}$$

Hence for a beam with the left end clamped and the right end inertially loaded, the frequency equation is given by Equation (3.19).

Note that the frequency equation can then be used to produce the modal shapes for beam under vibration. This is done by calculating the eigenvalues, β_n for n=1,2,…n. The eigenvalues can be found by computation algorithms involving iterative methods.

3.4 FINITE ELEMENT ANALYSIS OF THE ABSORBER

In order to gain an accurate prediction of the modes of the absorber, a numerical analysis using finite elements was used. This analysis allows determination of the resonance frequency of each mode, which will be a function of the location of the mass along the two shafts. Two main types of meshing elements (in Ansys) were used to model the absorber device. For the hollow square housing in the centre (which attaches to the vibrating surface), shell63 was used. The suitability of this element was based on its bending and membrane properties. For the modelling of the two shafts and absorber masses, SOLID45 tetrahedra was used. More detail can be found within the Ansys manuals. The boundary conditions were then programmed by fixing (in all directions) one side of the square housing . The final model of the device is shown in figure 3.7. Note that one of the shafts will be threaded and the other is smooth. A controller will be attached to the threaded rod. When it is turned, the end masses will move in or out.

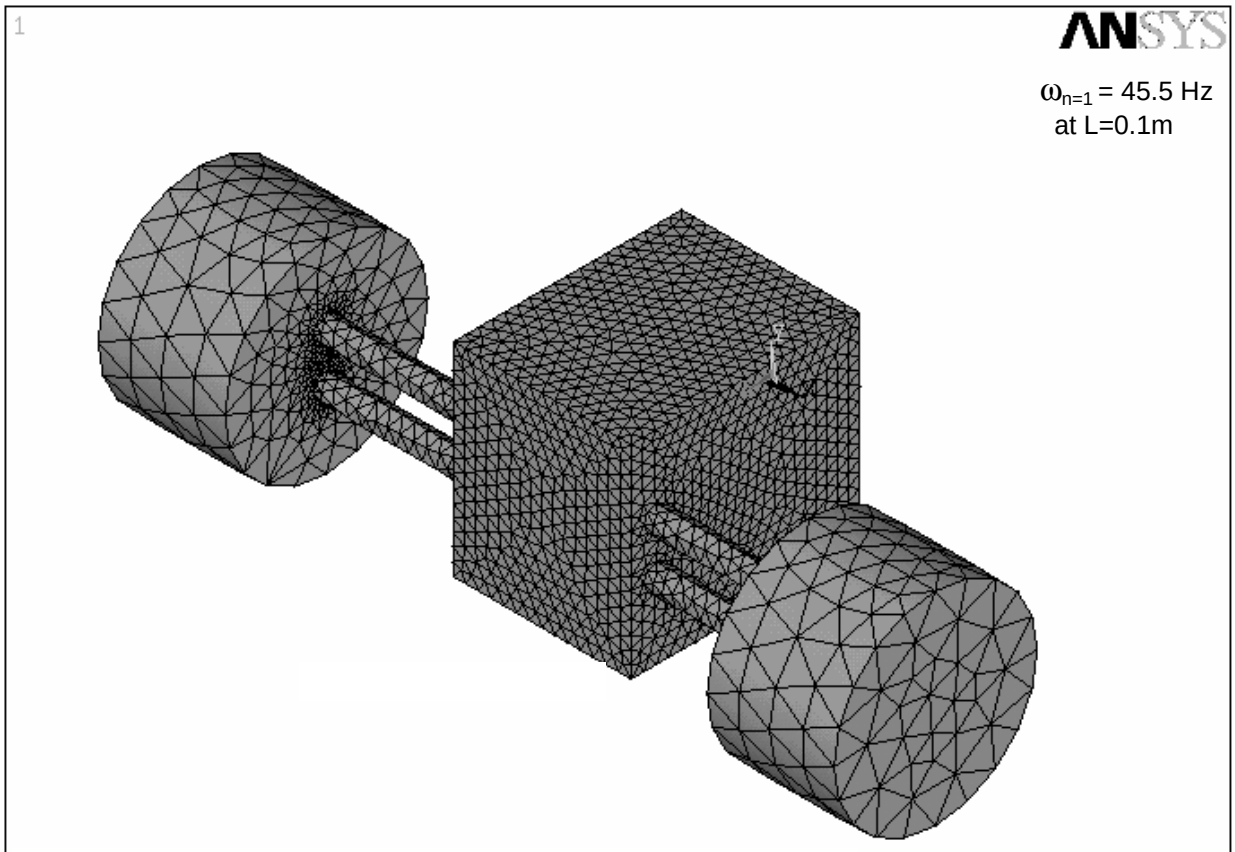

Figure 3.7 – A meshed model of the Dynamic Absorber

3.5 EXPERIMENTAL SETUP

3.5.1 Introduction

The experiments undertaken on the dual cantilevered mass absorber are performed in three setups:

1. Examining the resonance frequencies of the absorber alone when it is directly attached to a shaker.
2. Examining the resonance frequency and vibration attenuation achieved by the absorber when it is attached to the simply supported beam. At this stage the absorber is tested without the control system.
3. Examining the effectiveness of the control system and rate of adaptation when the absorber is attached to the beam.

3.5.2 Resonance frequency experimental measurement of absorber (alone)

To determine the natural frequency of the absorber (alone), the device was attached directly to a shaker and subjected to a variable frequency sinusoidal input (sine sweep). The transfer function was then taken between the point of attachment and the absorber mass.

The arrangement is shown in figure 3.8.

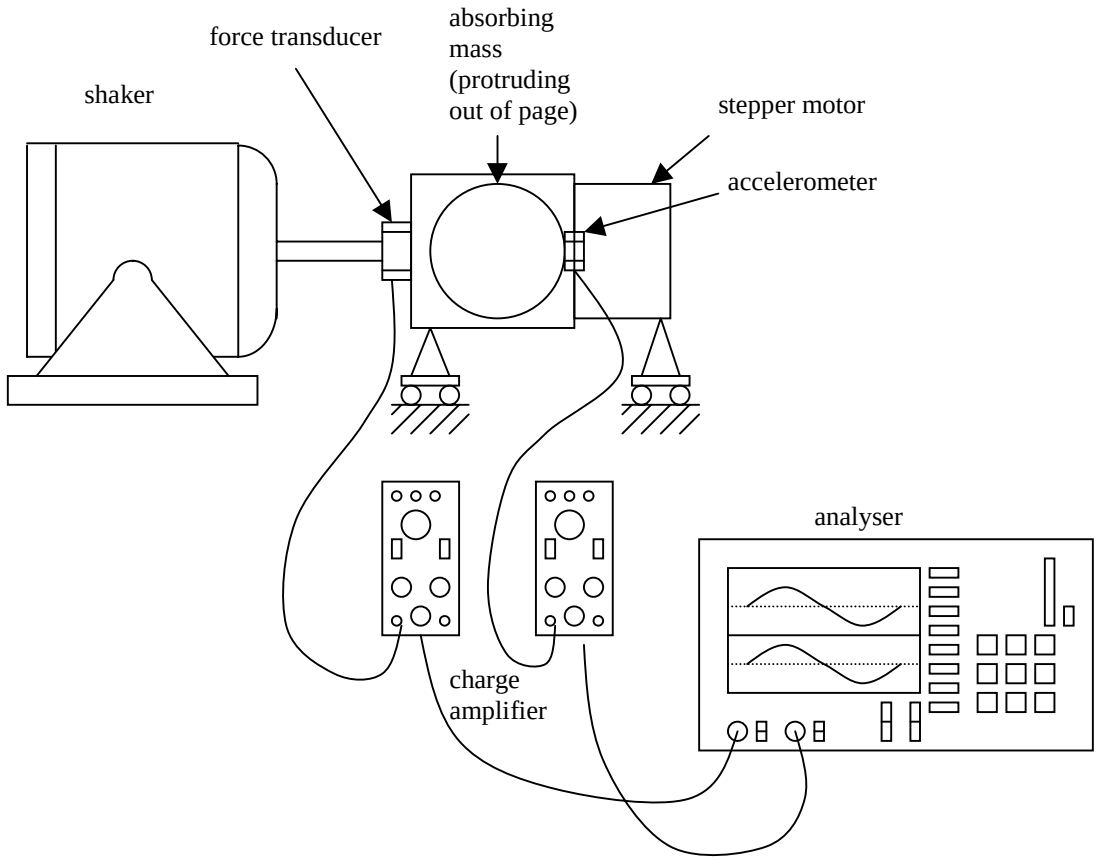

Figure 3.8 – Measuring the resonance frequency of the absorber alone

In the setup the absorber device is acting in a bending motion. That is, it acts as a uniform beam which has a force input in the centre, and is inertially loaded at both ends. The result obtained here will be different from the result obtained when the absorber is attached to the beam.

3.5.3 Experimental Results

The plot of the transfer function obtained from this setup is shown in figure 3.9. Note that three different curves are given, for the mass located at distances of 92mm, 98mm, and 105mm from the edge of the absorber base. (refer to figure 3.10 for datum point). This experiment verifies that the natural frequency of the absorber changes when the position of the mass along the rod changes. However, the values for the natural frequencies shown here on figure 3.9 do not span the full frequency range possible with the absorber. The full frequency range will be found when the absorber is later attached to the beam.

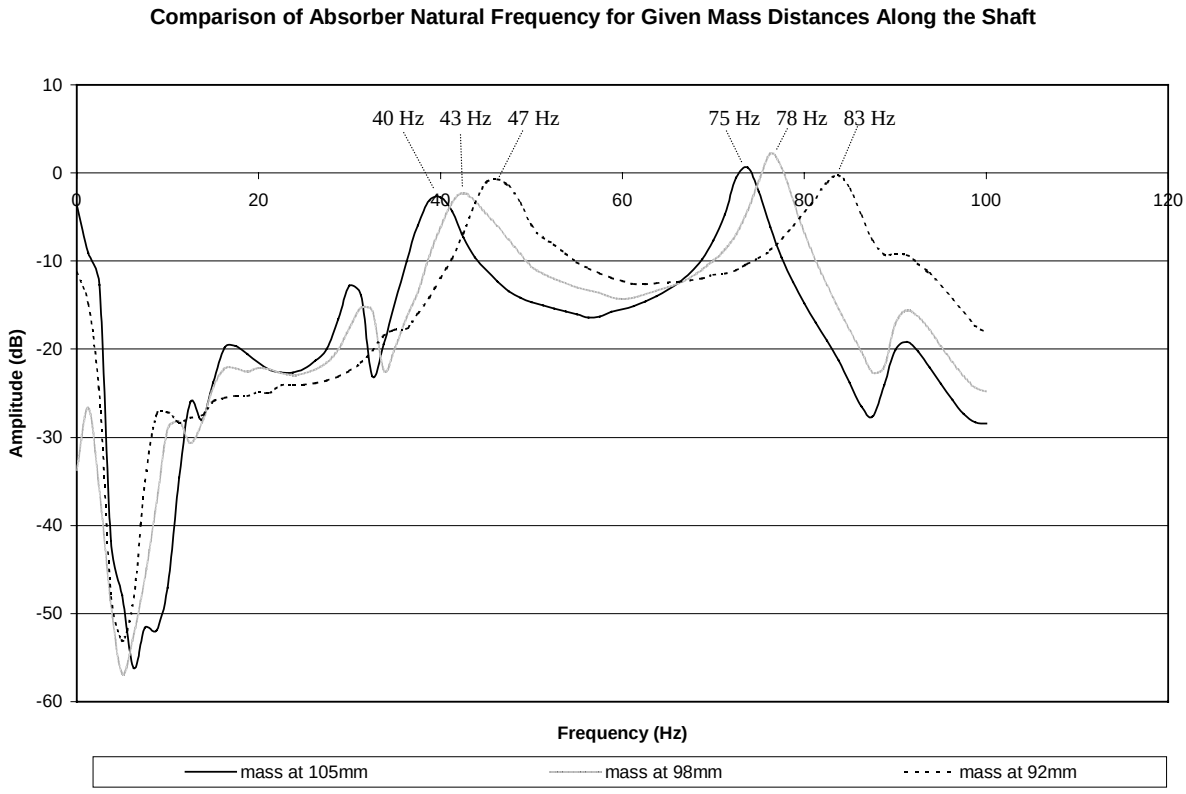

Figure 3.9 – Transfer function of the absorber

The absorber is tuned according to the number of steps turned by the stepper motor. The datum for the position is given by 0 mm at the point when the mass is up against the shell wall. This is illustrated in figure 3.10.

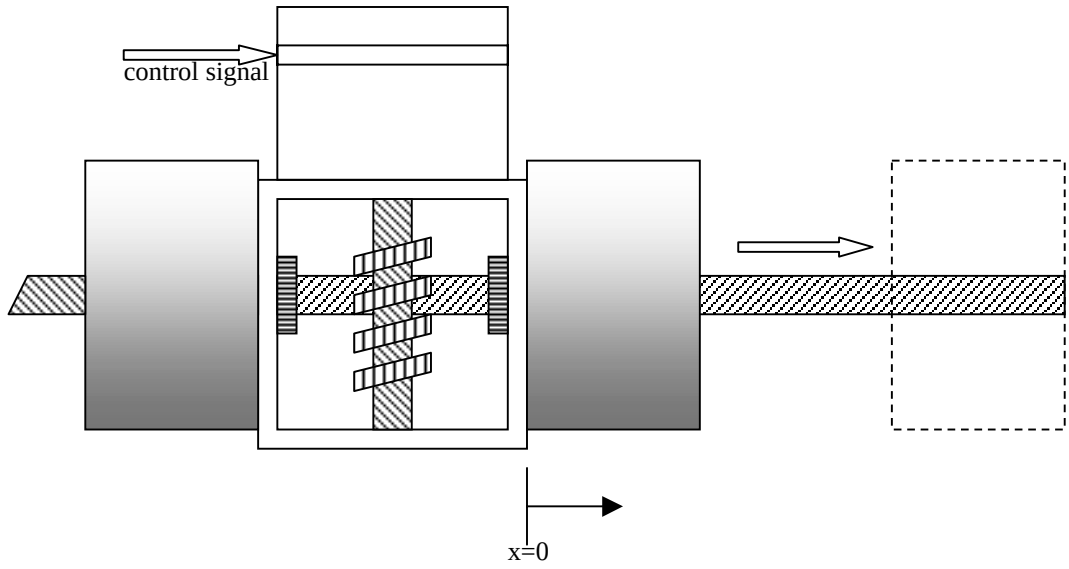

Figure 3.10 – Positioning for the number of turns made by the motor

The worm gear built within the device allows the absorber mass to be precisely tuned to the number of steps of the motor. Starting from the datum, at x=0, the number of steps is 0. For x=92mm, the number of steps required for the motor to turn is 80,000. For x=98mm the motor has to turn 100000 times, and for 105mm the motor is turned 120000 times. The peaks obtained from these values of turns is shown in the transfer function plot of figure 3.9 above. It can be seen that at 80000 turns the natural frequency of the absorber is at 47.0 Hz. At 100000 turns the natural frequency decreases to 43.0Hz and for 120000 turns, the corresponding value is 40 .0 Hz. These values are lower than those obtained when the absorber is fixed to the beam (discussed later). The theoretical analysis for the absorber when it is undergoing a bending motion is done in section 3.3. As the natural frequencies correspond to the number of steps, it is then possible to tune the absorber to any frequency within its range, by resetting the mass to its datum position whenever the device is mounted onto a structure.

The plot of the transfer function in figure 3.9 shows that the second mode of the absorber is around 80Hz; ω_{80k}=75.0Hz, ω_{100k}=78.0.0Hz, ω_{120k}=83.0Hz, for turns of 80000, 100000 and 120000 respectively. The second mode of vibration of the absorber is a twisting action as shown in figure 3.1. As this is not a bending motion, this mode is not effective in controlling the transverse vibration in the beam. It is possible that this second mode may contribute to the modal amplitude at frequency ω_{22} (as shown in figure 1.2) when the absorber is mounted on the beam. However, this will not affect the attenuation achieved by the absorber at the frequency of excitation.

3.5.4 Experimental setup with the absorber on the beam

In the second setup, the absorber device is acting as two cantilevers with a concentrated mass attached to the end of each. Each cantilever acts as a beam which is inertially loaded at one end and clamped at the other. The theoretical analysis of this has been described previously in section 3.3. The shaker is attached to the beam such that it is able to move along the beam for different point source locations. This will assist in the study of the effect of source location on the frequency response of the absorber. The absorber itself is attached to the beam via clamps. Similarly, this allows the location of the absorber to be changed to produce a favourable output signal from the accelerometer.

It is assumed that the fundamental mode of vibration contributes the most towards the overall vibration in the beam. The absorber is located slightly off-centre on the beam, to allow it to respond to the first and second modes of vibration. However, the second mode is not aimed to be controlled by the absorber in this experiment.

The setup is illustrated in figure 3.11.

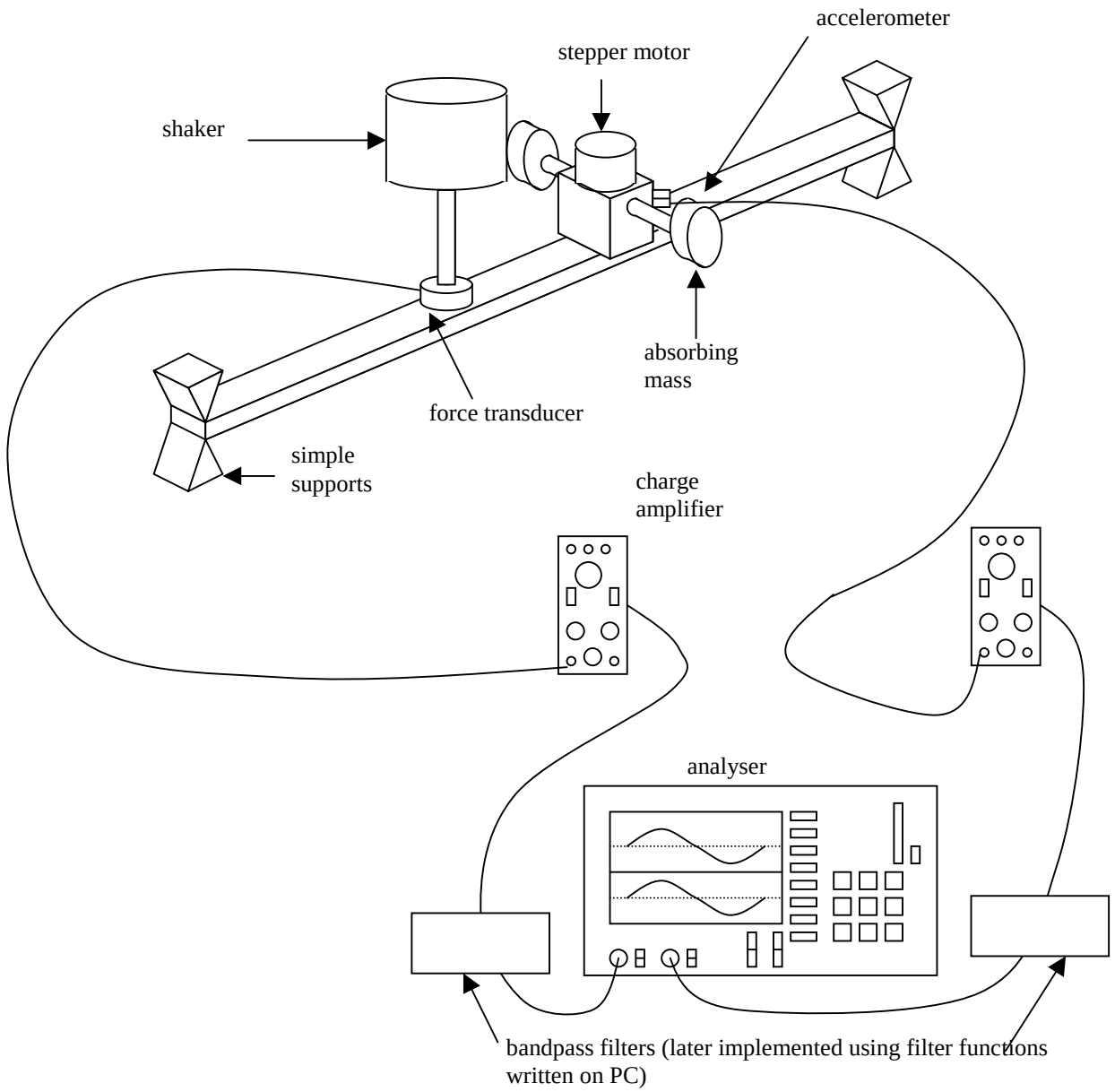

Figure 3.11 - Experimental setup for the absorber attached on the beam

The input force is measured by a force transducer placed between the shaker stinger and the point of attachment on the beam. The acceleration level of the absorber mass is measured by an accelerometer placed on top of the mass. This accelerometer is located on the horizontal plane tangential with the top of the absorber mass. This is to ensure that the acceleration recorded by the accelerometer does not include any longitudinal movement of the mass along the horizontal axis.

The transfer function is calculated by dividing the input level from the force transducer over the input level from the accelerometer, thus giving a ratio $F_{input}/a_{absorber\ mass}$.

The following properties were used for the simply supported beam.

Property	**Value**
Length, l	1.135m
Height,h	0.05m
Width,b	0.025m
Modulus of Elasticity, E	207×10^9 Pa
Density, ρ	7800 kg/m^3
Second Moment of Inertia, I	bh^3/12

The length of the beam was arbitrarily chosen such that the resonance frequency of the beam would be near the operating range of the absorber. This value was calculated using Euler equations for beams.

The fundamental frequency for a simply supported beam is given by,

$$\omega_1 = (\beta l)^2 \sqrt{\frac{EI}{\rho A l^4}} \qquad for \qquad (\beta l)^2 = 9.87$$

For $$I = \frac{bh^3}{12} = \frac{0.025\times0.05^3}{12} = 2.6\times10^{-7}\, m^4$$

and $$\rho A = 9.75 kg/m$$

$$\omega_1 = 9.87\sqrt{\frac{207\times10^9\times2.6\times10^{-7}}{9.75\times1.35^4}}$$

$$= 402 rad/s$$

$$= 64 Hz$$

This measured value for the beam resonance (at this length) is expected to be greater than this value.

3.6 CONTROL SYSTEM

3.6.1 Controller setup

The aim of the work described in this thesis is to produce an absorber which is tunable “on-line”, to provide an alternative to the actuators currently used in active vibration control and structural / acoustic control. Adjustment of the resonance frequency of the cantilever beam absorber can be made via adjustment of the location of the masses on the shafts.

The hardware used to facilitate movement of the absorber mass in and out on the shafts consists of a stepper motor and a CIO-DIO (digital input-output) card. The stepper motor is connected to the main shaft of the mass by a set of worm gears. The digital input-output card is inserted into a standard ISA port on a Pentium PC running at 150 MHz. The PC is used to control both the controller card and the data acquisition card.

As will be described in detail later, the software used to control the card was written in C++ using the National Instruments package, Lab Windows. The flow of control signals is illustrated in figure 3.12.

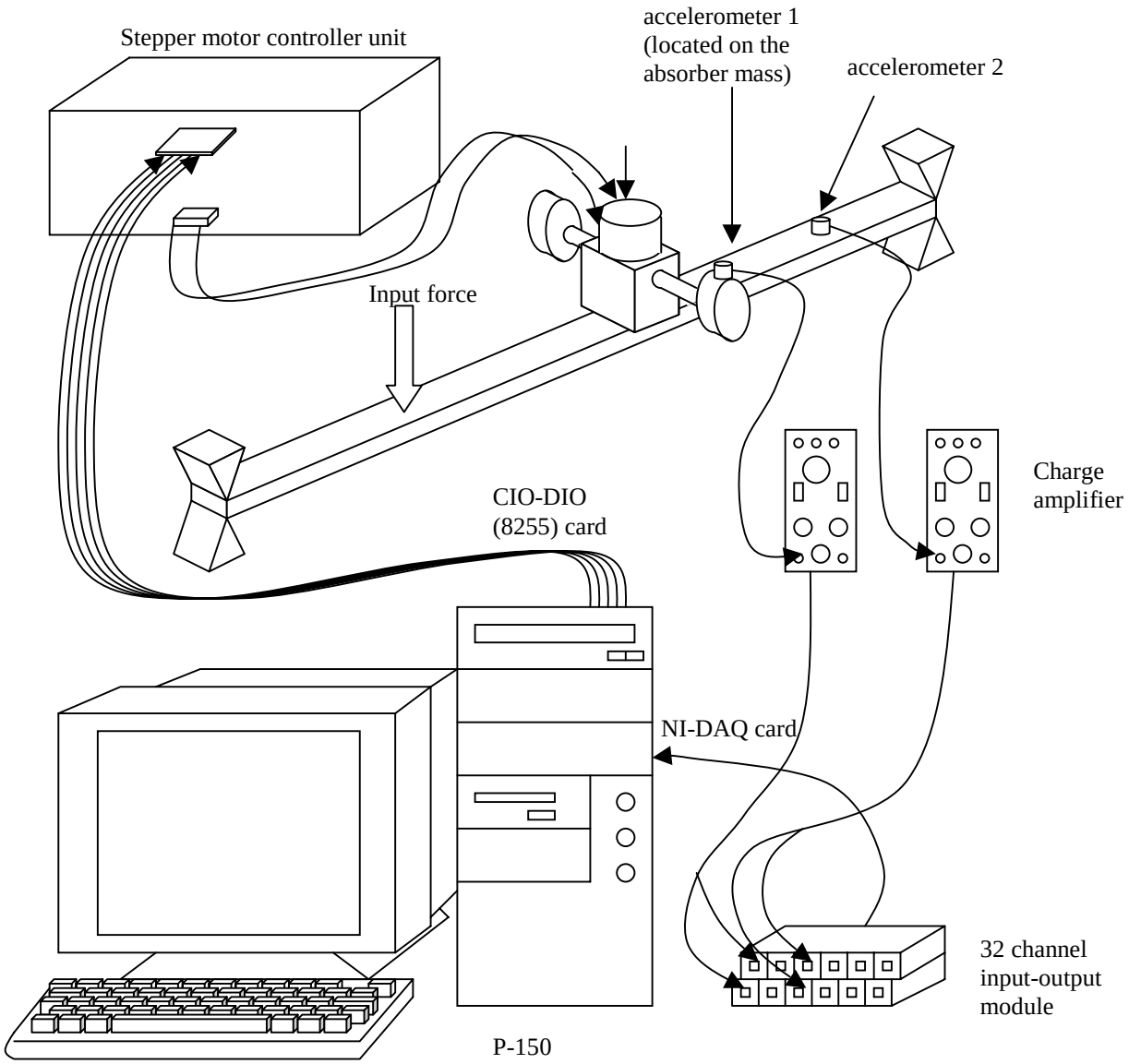

Figure 3.12 – Control Signals

For the purposes of experimental analysis of the absorber device (itself, as opposed to the overall control strategy), the stepper motor was initially driven using a simple program written in C++. The program is included in Appendix B. The stepper motor operates by a series of pulses or "steps". A step is triggered when a signal changing from 0v to 5v is detected by the motor. Thus by sending a series of pulses ranging from 0-5v, the motor can be precisely controlled in terms of movement through a number of steps.

The program first sets the hexadecimal base address of the CIO-DIO card to 1b0. Then according to user input, it sets the direction for the motor to turn by sending a word to certain addresses above its base address. A word consists of 8 bits which can be turned on or off, depending on the operation which is required by the stepper motor. A loop is then set up to generate the required number of pulses to turn the motor a given number of steps.

There are 2 accelerometers used in the system; one located on the absorber mass to determine the natural frequency at which the absorber is tuned, and the second is attached to the beam to measure the excitation frequency.

3.6.2 Tuning Algorithm

Vibration absorbers are typically tuned in one of two ways; either to a modal eigenfrequency which is some cause of concern, or to a disturbing frequency, which may vary over the whole spectrum of the primary structure. In the first case, unless the primary structure undergoes some change in its internal properties, due to time or temperature effects, then there would normally be no need for an adaptive absorber. In this work, the tuning laws will be written to track the excitation or disturbance frequency; this will have more practical use.

In designing the tuning algorithm for the absorber device, it is important to note the areas of delay in which absorber adaptation are normally related (Von Flotow, 1994). Firstly, there is the logic delay. This is the time required for the feedback control system, in this case the computer program, to process any acquired data and give a response to the incoming information. Although a P-150 computer is used as the main hardware for the flow of control signal, it has to perform the simultaneous processing of the incoming and outgoing information. It is possible that this will contribute significantly to the overall delay of the control system. With the presence of noise in the incoming signal, this delay will be further increased, as more time will be required for averaging, filtering and further iterative processes within the algorithm.

Secondly, there is the actuation delay. This is the time taken for the absorber device to change its internal properties so that it is adapted to the changing environment. In this case, this is the time required for the absorber mass to move to a specified position which will change its eigenfrequency to match the excitation frequency. It is anticipated that this will be the main area of delay, as this is the compromise which has to be made for a device which has a fine-tuning ability.

Finally, there is the dynamic delay. This is the time required for the device to change its state of vibration once it is tuned to those conditions of the primary structure. The dynamic delay is proportional to the quality, Q, of the absorber, and is often represented by a time constant (Von Flotow, 1994),

$$\tau_{dynamic} = \frac{Q_a}{\pi} \ (periods) \qquad where \ \ \tau_{dynamic} = dynamic \ \ delay \ \ \exp ressed \ \ as \ \ an \ \ \exp onential$$

$$Q_a = quality \ \ factor \ \ of \ \ absorber$$

It can be seen that the dynamic delay will decrease if the damping coefficient is increased. However, this results in residual motion of the primary structure even when the absorber is perfectly tuned. Because of this, it is usual to decrease only the first two forms of delay, and maintain the quality of the absorber at a high value. Dynamic delay is normally considered negligible compared to the logic and actuation delays. The dynamic delay also includes the time required for the primary structure to respond to changes in the absorber.

The program written to control the input and output signals can be seen in Appendix B. It is written under the Windows NT4 environment using the National Instruments package CVI (C for Virtual Instrumentation). Because this program has numerous built in functions, the use of low-level Data Acquisition libraries could be incorporated directly into the program. The overall process for the feedback algorithm can be shown in figure 3.13.

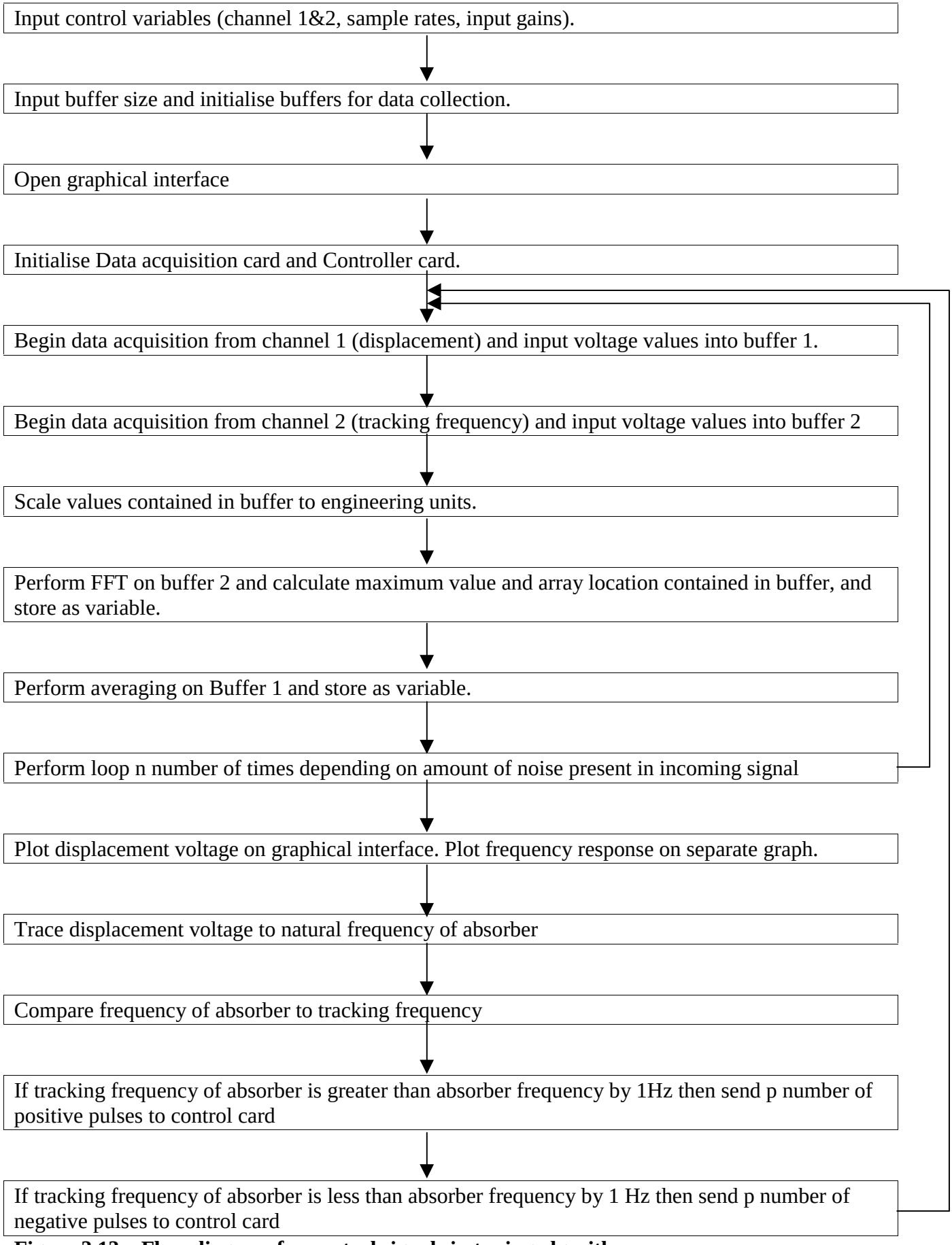

Figure 3.13 – Flow diagram for control signals in tuning algorithm

3.6.3 The Linear Transducer

The position of the absorber mass at any point in time is known by incorporating a linear transducer into the design of the device. This linear transducer consists of a rotational pot which gives out a voltage variation depending on the number of turns it has completed. A torsional spring is built into the transducer so that it will recoil whenever the absorber mass is moving inwards along the rod. The pot is connected to one of the masses via a string which is glued to the surface. The arrangement can be shown in figure 3.14.

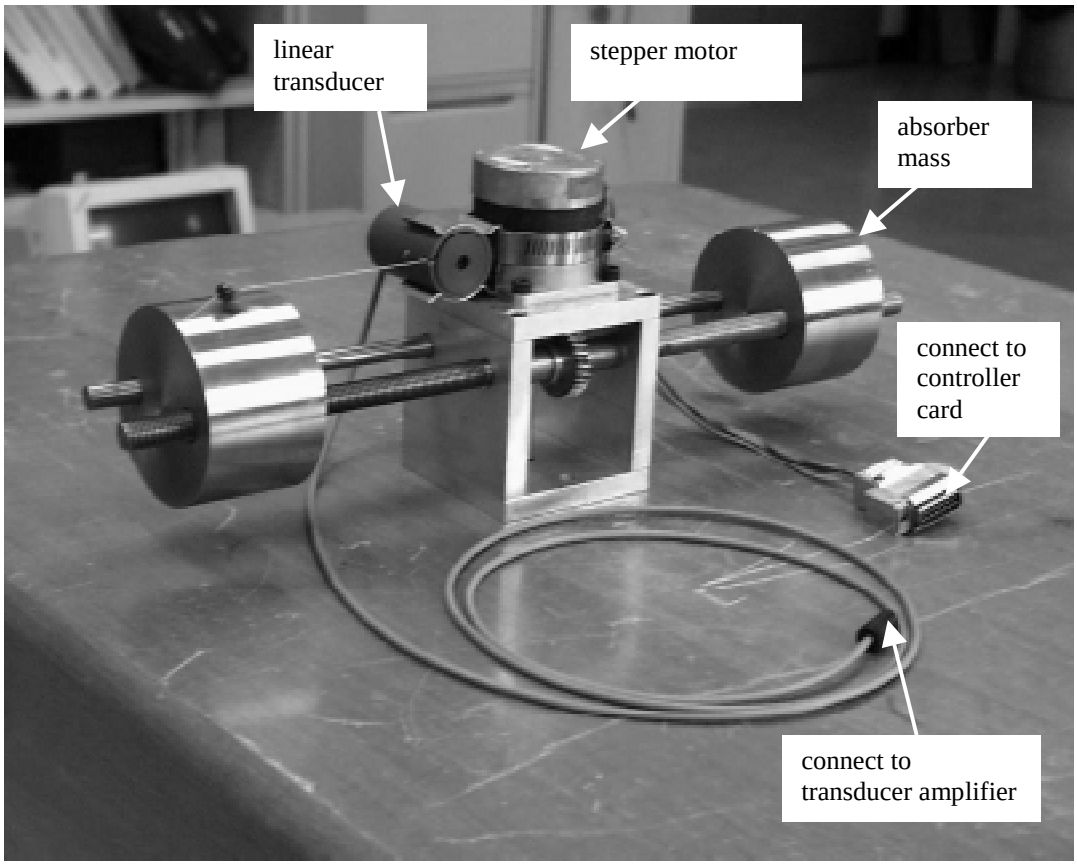

Figure 3.14 - Location of the Linear Transducer

The output of the transducer is passed through a power amplifier and the signal is converted to a DC voltage and then into the NI-DAQ card.

Figure 3.15 shows the relationship between the voltage produced from the linear transducer and the natural frequency of the absorber.

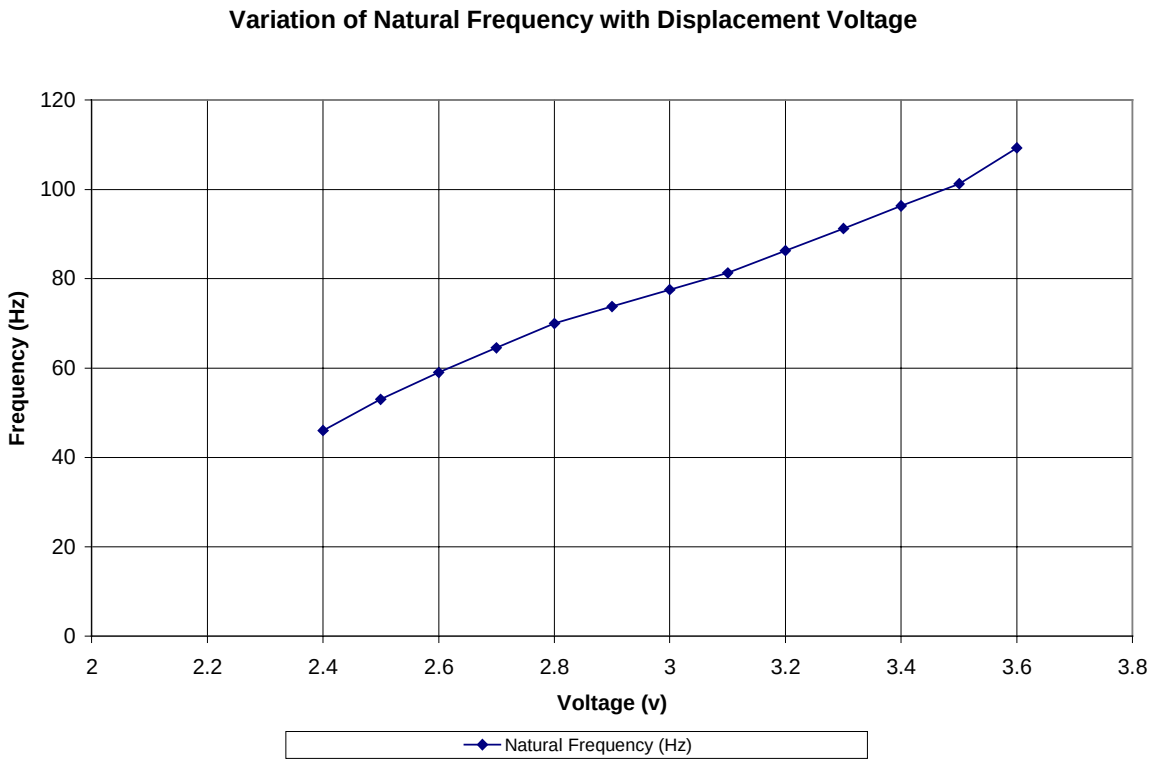

Figure 3.15 - Variation of Natural Frequency with Displacement Voltage

Figure 3.15 shows that there is a linear relationship between the voltage output from the transducer and the natural frequency of the dynamic absorber. It is because of this linear relationship that a proportional controller can be written into the tuning algorithm. The target frequency is measured from the sensor, which tracks the excitation frequency. From this, a precalculated voltage is known, which is the target value for the output voltage from the linear transducer. The stepper motor is then actuated to move the masses in either direction, until the values for both the calculated and output voltage coincide. The sensitivity of the absorber can be adjusted by defining the tolerance between the calculated and output voltage. When the difference between the two voltages is greater than the tolerance, then the motor is actuated.

3.7 EXPERIMENTAL RESULTS FOR THE CASE OF THE ABSORBER MOUNTED ON THE BEAM

3.7.1 Performance of the absorber on a sinusoidally excited simply supported beam

Figure 3.16 shows the transfer function obtained from the second setup in section 3.5.4.

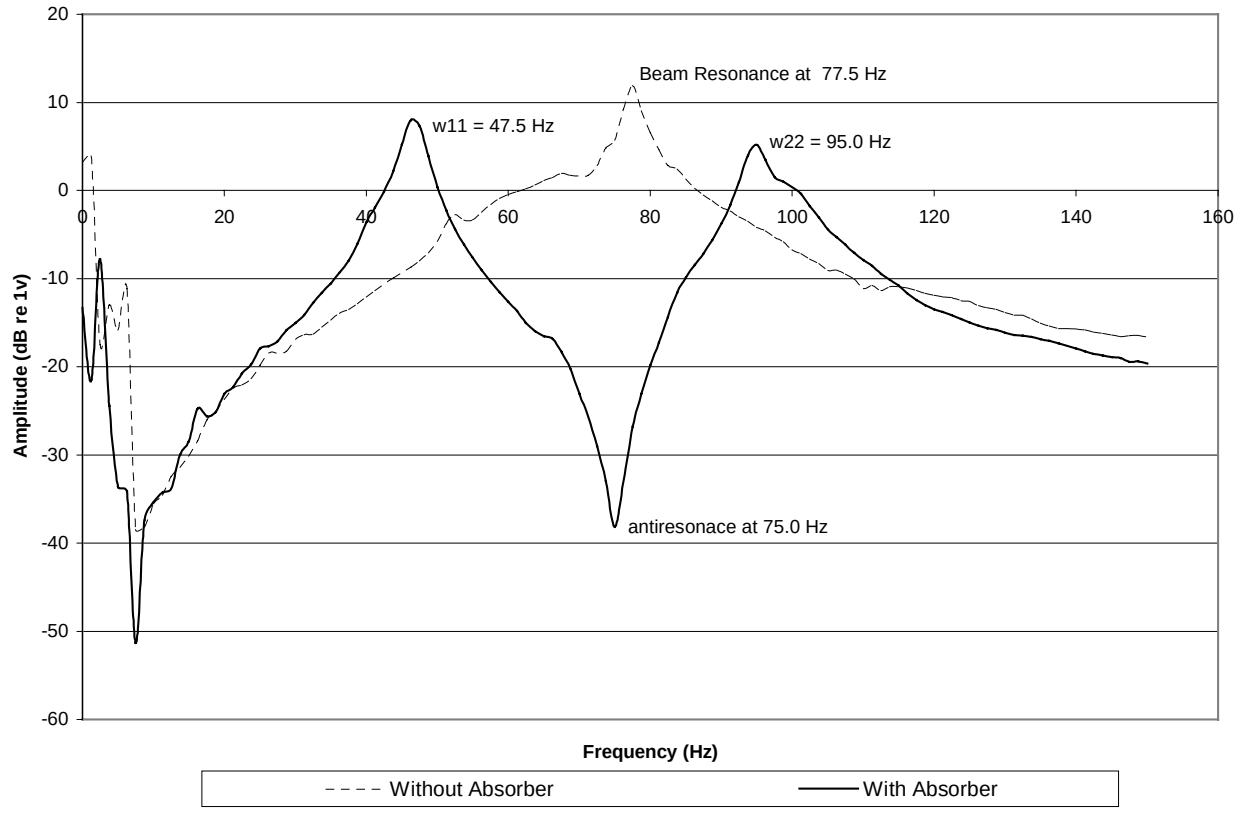

Figure 3.16 – Transfer function before and after absorber installation

Figure 3.16 shows the fundamental frequency of the beam at 77Hz, without the absorber mounted. This value is higher than the calculated value using the Euler equation, due to the discrepancies in the beam terminations. The boundary conditions achieved at both ends of the beam in the experiment suggests a range between a simply supported termination ($f_{n=1}$=64 Hz) and free-free ($f_{n=1}$=206 Hz). The scale is calibrated for 1 dB relative to 1 N/m/s^2.

When the absorber is mounted on the beam and self-tuned to remove the peak, it can be seen that an antiresonance is produced near the frequency at which the resonance previously occurred. This results in the amplitude of response at the target frequency being attenuated by approximately 45dB. This indicates that the dual cantilevered mass absorber, when correctly tuned has the capacity to substantially reduce the vibration in the beam.

3.7.2 Variation in natural frequency of the absorber due to change in effective rod length

Illustrated in figure 3.17 is the change in frequency responses of the absorber / beam system as the absorber mass is moved along the rod. The transfer function is taken between the source and at a point along the beam as shown in figure 3.12 using accelerometer 2.The antiresonance produced had a range from 45 Hz up to approximately 90 Hz. At lower half of this range the antiresonances were sharper. This is due to the damping in the absorber being frequency dependent. When the mass is positioned 30mm from the base, the frequency of the absorber is at 88 Hz. At distances of 70 mm and 110 mm the frequencies are 65 Hz and 45 Hz respectively.

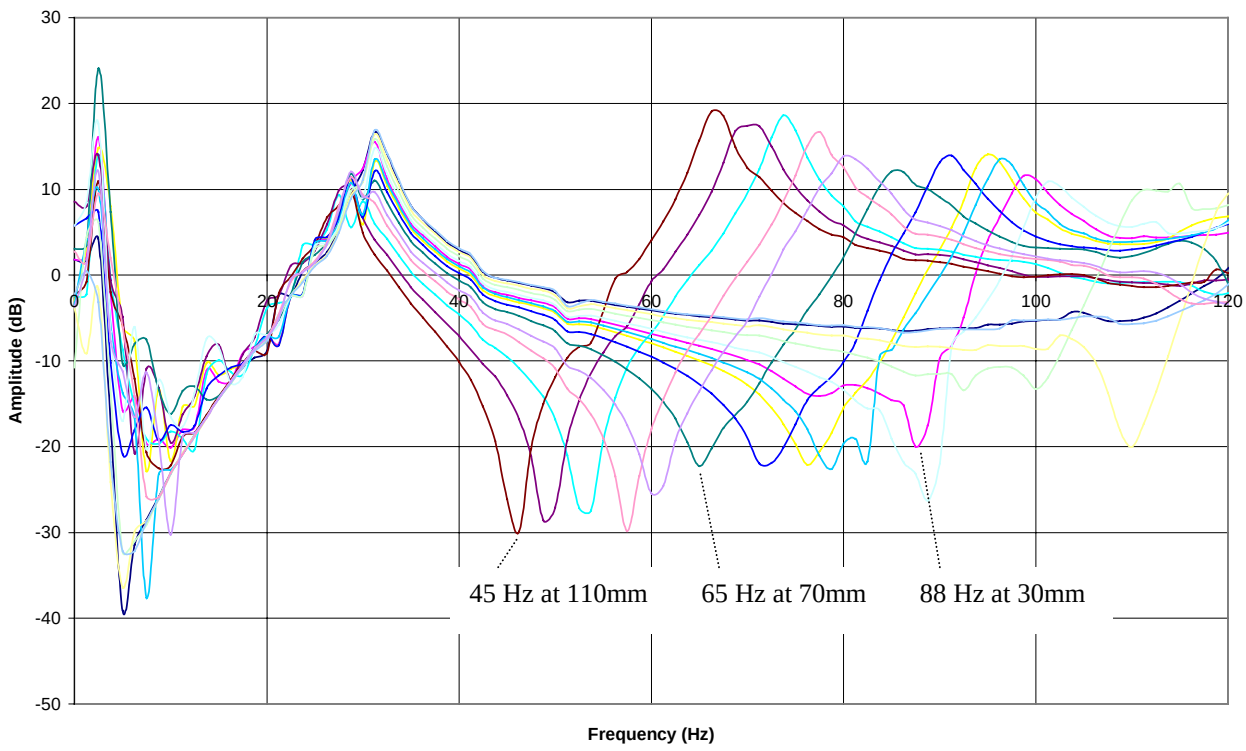

Figure 3.17 - Comparison of anti-resonances produced due to change in absorber

3.7.3 Speed of Adaptation

For tests in the frequency range of interest here, attachment of the absorber to the vibrating beam resulted in an attenuation of approximately 30dB. (This was when the absorber was located in a position slightly off centre). The time varying signal from the sensor to measure the amplitude of the vibrating beam taken from an accelerometer located near the point of attachment can be seen in figure 3.18.

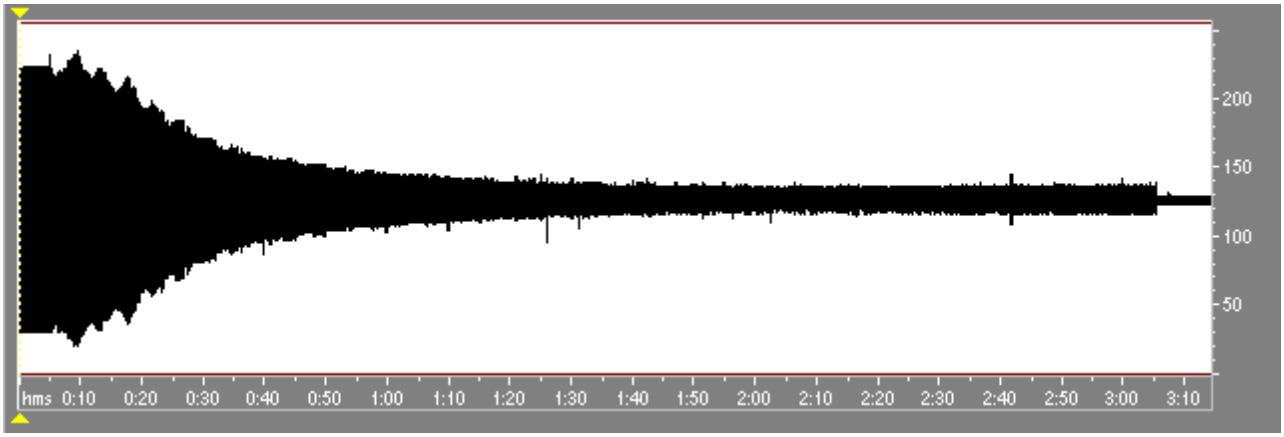

Figure 3.18 – Time signal for absorber to adapt to a changing excitation signal

Figure 3.18 shows the time required for the absorber to adapt to an excitation signal. In this case, the absorber is initially tuned to a frequency of 46 Hz. This frequency is chosen arbitrarily as it is in the lower end of the operating span of the absorber. The excitation frequency is then increased to 72 Hz and at t=7sec, the controller program is run. The distortion which can be seen starting at t=7 sec is due to the small vibration caused by the stepper motor itself. This external noise does not interfere with the tuning algorithm since the resonance caused by the motor is at a frequency ω_e = 250Hz (recall that there is a band-pass filter on the sensing signal).

The vibration amplitude decreases to about 20% of original at about t=60 sec. This time is highly dependent on the span of the frequency change. The overall tuned amplitude of the beam is only known once the absorber stops tracking. In this case this occurs at t = 3min 5 sec. A slight drop in amplitude can be observed at this time when the motor stops tuning.

Figure 3.19 shows the response of the adaptive absorber when the frequency is changed twice from an initial frequency of 92 Hz to 75Hz and then down to 52 Hz. This is to test the response time of the absorber over the whole span of its operating frequency.

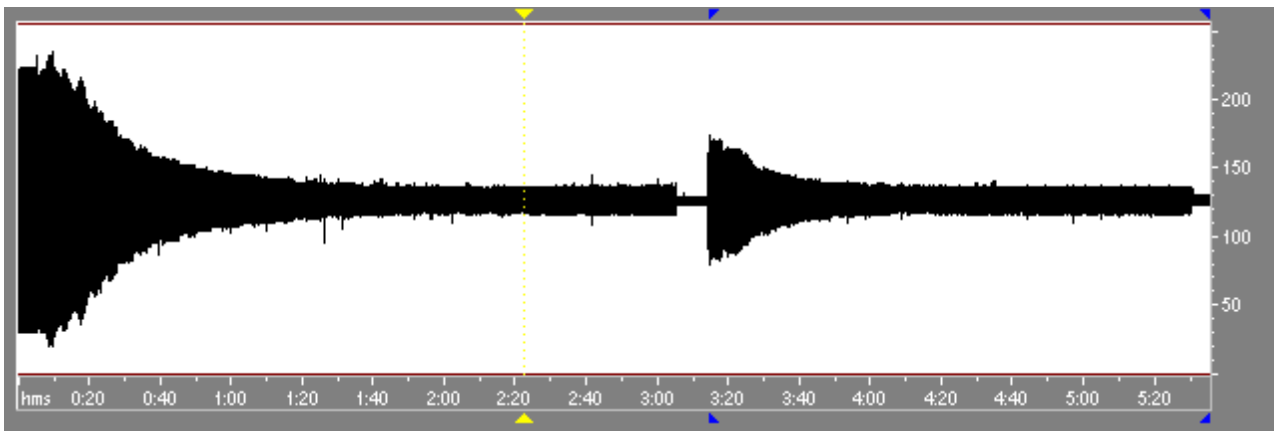

Figure 3.19 – Time signal for absorber to track 2 changing excitation frequencies in succession

It can be seen that when the motor is turned on, there are small fluctuations in the signal. This does not affect the performance of the absorber as the controller is working in the frequency domain. A band-pass filter has been incorporated into the controller program to overcome the interference from external disturbances. When the signal which is being tracked (the excitation signal) reduces such that the amplitude of the external disturbance is greater, the band-pass filter aims to prevent the controller from tracking to the disturbance signal.

3.8 SUMMARY

In this chapter, an improved dynamic vibration absorber has been designed and tested, using a cantilevered mass arrangement.

Theoretical analysis has been undertaken to predict the behaviour of the absorber using discrete and continuous system methods. A more accurate analysis has been done using finite element analysis to calculate the operating range of the absorber design.

The performance of the absorber has been tested on a simple base structure, and an adaptive component has been incorporated into the design. The limitations discovered from the first and second prototype of the dynamic absorber have been addressed:

1. The operating range of frequencies for the cantilevered absorber has been improved. The practicability of the absorber is thus improved.
2. The damping associated with the dynamic absorber has been reduced, thus improving the maximum level of attenuation possible when the absorber is mounted onto a beam.

The absorber has been shown to be able to effectively reduce the vibration in a beam.

A tuning algorithm has been written for the absorber to track a single frequency disturbance on a simply support beam. A “front end” has been written so that the absorber can be used “on line”.

The rate of adaptation achieved when using a simple proportional tuning algorithm has been tested for the absorber. The response time has been shown to be highly dependent on the difference between the current and target frequencies.

CHAPTER 4 SUMMARY AND CONCLUSIONS

4.1 SUMMARY OF DYNAMIC ABSORBER USING ENCLOSED AIR

This study has demonstrated that enclosed air can be used as an effective mechanism to achieve the stiffness component required for a Dynamic Vibration Absorber. For controlling vibration at a single frequency, the air-spring absorber is a viable device.

In the design of the enclosed air-spring absorber, the stiffness provided by the air has been shown to correlate with the theoretical model for an enclosed volume. For the rubber diaphragm absorber, the value of stiffness deviates from the theoretical value when the height of the enclosed volume is less than 60mm. Problems such as lack of pressure (within the enclosed volume) and frequency span have been addressed with the aluminium diaphragm absorber.

The level of attenuation achieved using the air-spring is in the order of 10 dB, due to the damping present in the absorber. This problem is addressed by the design of the cantilevered-mass absorber.

4.2 SUMMARY OF DUAL CANTILEVERED MASS ABSORBER

In this study, an adaptive dynamic vibration absorber has been designed using a dual cantilevered mass arrangement. This absorber is effective in controlling single frequency vibration on a simply supported beam. The controller for the absorber has been designed and constructed, and the control algorithm has been derived for the adaptive component. The adaptive system has been found to be effective in tracking a changing excitation frequency, with minimal error and guaranteed stability.

4.3 FUTURE WORK

4.3.1 Future work for the air-spring absorber

1. The air spring absorber has potential to be used for adaptive vibration control. An adaptive component similar to that used for the cantilevered absorber can be incorporated into the design of the air-spring absorber, by connecting the piston to a stepper motor and feedback system.

2. The limitations imposed on the absorber in this study due to material properties can be addressed. The construction of the diaphragm can be moulded such that there is minimal distortion when the pressure increases. This can also be used to minimise the rotational effect on the absorber mass.

3. To achieve a greater frequency span, the air-spring absorber can be pressurised. However, this will add cost to the device, and maintenance will then be required on the absorber.

4.3.2 Future work on the dual cantilevered mass absorber

1. Presently, the control system for the absorber is connected to a PC and various controller hardware. It is planned to have the adaptive component programmed into a Programmable Logic Controller or some other microprocessor-based platform. This will reduce the size of the electronics required to implement the adaptive absorber, and make the device more portable. The cost of the overall system will also be reduced.

2. There are plans for the absorber to be used to control the vibration on an electrical transformer. Research is required to determine how effective the absorber will be when attached to a system with a much greater equivalent mass.

3. For an absorber-based approach to noise and vibration control on a complex system, multiple absorbers will have to be used in conjunction with one another. Work is required to determine different configurations and placements of the absorbers. Absorbers can also be tested in conjunction with other forms of vibration control, such as active means. Multiple absorbers can also be used to target higher resonance frequencies on the structure.

4. Presently, the dual mass absorber is effective in controlling vibration along one axis. By combining another two masses in line perpendicular to the present shaft, the absorber-array device can be used to control vibration on a multiple axis / multiple frequency configuration.

CONCLUSION

In this study, two different absorber arrangements have been investigated, both demonstrating potential to be used in vibration control.

An air-spring absorber has been designed using enclosed air to provide the spring stiffness. With this absorber, the enclosed air mechanism has been shown to provide an acceptable frequency span. The performance of this absorber is acceptable in reducing the vibration on a simply supported beam.

A dual cantilevered mass absorber, which uses cantilevered beams and concentrated masses, has demonstrated to be very effective in controlling the vibration in a simply supported beam. This arrangement has been shown to be capable of being incorporated for adaptive use. Effective attenuation has been achieved with this absorber and further work will be planned for this device.

APPENDICES

Appendix A Ansys Program

Appendix B Stepper Motor Program

Appendix C CVI Program for the feedback control system

Appendix D Illustrations

Appendix A Ansys Program

```
! This is a program which models an adaptive absorber fixed to
! a beam as a vibration control device.
! The absorber can later be tested on a transformer for noise
! control purposes.

/batch

/filname,absorber1
/title, Dual Mass Dynamic Absorber
/units,SI

! Suppress comments from output files
/PAGE,10000,,10000
! Expand output file fields to avoid fields overlapping
/FORMAT,,,15,6

!_____________________________________________________________________

!
!  SYSTEM GEOMETRY
!  ====== ========
!                 PLAN VIEW
!
!                          |----rodleng----|
!
!   _____          __________          _____   ____
!  |     |________|          |________|     |  |
!  |      ________            ________      |  |  massdiam
!  |     |        |          |        |     |  |
!  |     |________|          |________|     |  |
!  |      ________            ________      |  |
!  |_____|        |__________|        |_____|  _|__
!
!                 |--xleng--|
!                                  --|     |-- massleng
!
!


! Define Solid Model Parameters

! Properties for Steel
stdens = 7800           ! density of steel = 7800 kg/m3
stE = 207E9       ! Elastic modulus  = 207 GPa
stG = 79.6E9            ! Shear modulus    = 79.6 GPa
stpois = 0.3            ! Poissons Ratio   = 0.3

! Properties for Center Square Section (CSS)
sthick = 2E-03          ! shell thickness  = 2mm


! FE Model parameters

lelsize = 0.02          ! element size
melsize = 0.1           ! meshing size

! CSS Dimensions
xleng = 0.07
yleng = 0.08
```

```
zleng = 0.08

! Rod Dimensions
roddiam = 0.01
rodleng = 0.145

! Absorber Mass Dimensions
massdiam = 0.080
massleng = 0.050

!_____________________________________________________________________

! Preprocessor
/prep7

! Define Material and Elements

! Shell elements

! The first element type is chosen to be shell63. This element has
! both bending and membrane capabilities. The key option 7 for
! this element is set, for reduced mass matrix formulation. The
! rotational degree-of-freedom terms are deleted. This is useful
! for improved bending stresses in thin members under mass
! loading.

ET,1,shell63
keyo,1,7,1

! Properties for the Center Square Section
r,1,sthick        ! defines the elements real constants
mp,ex,1,2.05E11   ! defines the linear material properties
mp,dens,1,7930
mp,nuxy,1,0.3


! Solid elements

!The second type of element chosen is solid45.

ET,2,solid45

! Properties for the Rod and Mass
mp,ex,2,2.05E11
mp,dens,2,7930
mp,nuxy,2,0.3


/COM, Generate the Solid Model

BLOCK,-xleng/2,xleng/2,-yleng/2,yleng/2,0,zleng+roddiam


! Cross Rod upper

! The FLST command specifies the data required for the picking
! operation. The 3rd field parameter is chosen from each of the
! subsequent command lines. 3 items are specified to be picked.
! 8 indicates that the items are to be of coordinate location
! type. The 9 constants are executed when p51X is declared.

FLST,3,3,8
```

```
FITEM,3,-rodleng,roddiam,zleng
FITEM,3,-rodleng,0.0126,zleng
FITEM,3,-rodleng,roddiam,zleng + roddiam/2

! A working plane is defined to assist in picking operations.
WPLANE,-1,P51X    ! negative value lets the user keep the
! present viewing direction
CYLIND,roddiam/2, ,massleng,2*rodleng-massleng,0,360,

! Cross Rod lower left
FLST,3,3,8
FITEM,3,-rodleng,-roddiam,zleng
FITEM,3,-rodleng,0.0126,zleng
FITEM,3,-rodleng,-roddiam,zleng + roddiam/2
WPLANE,-1,P51X
! Create cylinder model
CYLIND,roddiam/2, ,massleng,rodleng-xleng/2,0,360,

! Cross Rod lower right
FLST,3,3,8
FITEM,3,-rodleng,-roddiam,zleng
FITEM,3,-rodleng,0.0126,zleng
FITEM,3,-rodleng,-roddiam,zleng + roddiam/2
WPLANE,-1,P51X
CYLIND,roddiam/2, ,rodleng+xleng/2,2*rodleng-massleng,0,360,

! End Mass Left
FLST,3,3,8
FITEM,3,-rodleng,0,zleng
FITEM,3,-rodleng,0.0126,zleng
FITEM,3,-rodleng,0,zleng + roddiam/2
WPLANE,-1,P51X
CYLIND,massdiam/2, ,0,massleng,0,360,

! End Mass Right
FLST,3,3,8
FITEM,3,rodleng-massleng,0,zleng
FITEM,3,rodleng-massleng,0.0126,zleng
FITEM,3,rodleng-massleng,0,zleng + roddiam
WPLANE,-1,P51X
CYLIND,massdiam/2, ,0,massleng,0,360,

! Reset working plane
WPCSYS,-1,0

! Merge all volumes
BOPT,NUMB,OFF           ! Suppress warning message
VSEL,ALL                ! Select all Volumes
VSEL,U,VOLU,,1          ! Deselect Volume 1
! The VGlue command generates new volumes by gluing volumes so
! that they share areas along their common boundaries.
VGLUE,ALL
VSEL,ALL
! The Vovlap command generates new volumes which encompasses the
! geometry of all the input volumes defined by regions of inter-
! section.
VOVLAP,ALL

! Plot volumes in Isometric mode
/VIEW,1,1,1,1
VPLOT
```

```
! Tidy up data base
allsel
nummrg,kp   ! merge equivalent or coincident terms
save
fini

eshape,1          ! associate the element type with the volumes
lsel,s,loc,x,rodleng-massleng,rodleng     !line select start from
                                                ! x location
lsel,a,loc,x,-rodleng,massleng-rodleng
lesize,all,,,5          ! Apply divisions for meshing

lsel,inve
lesize,all,5e-03
lsel,s,loc,x,-xleng/2,xleng/2
lesize,all,15e-03
type,1
real,1
mat,1

vsele,s,volu,,10
aslve,s
amesh,all
type,2
real,2
mat,2
vsele,all
vsele,u,volu,,10
vmesh,all

nsel,s,loc,z,0
d,all,all
allsel
save
fini

/solu
! Choose the analysis type. For the modal extraction method,
! choose the subspace iteration method up to the 5th mode.
antype,modal
modopt,subsp,5
solv
fini
```

Appendix B Stepper Motor Program

```
//   Program to drive a stepper motor using an CIO-DIO 8255 board.
//   Control of the board is made through Port 2 on the card.
//   Please set the Base address to 1b0 Hex, or 432 Dec.


/* Includes */

#include <stdio.h>
//#include <lowlvlio.h>
#include <utility.h>
//#include <stdlib.h>

//void delay(double);
//void outp(int portid, int value);
//int inp(int portid);

/* Main */

void main(void)
{

const static base = 432;

int x,y,w,i,lmt1,u,f=3,r,value=144,port=base+3,port_2=base+7,port_3=base+4 ;
double z,s;

//clrscr();

for (i=1;i<=20;++i)
      {
      printf("\n");
      }

printf("Select Motor Direction\n");
while (f>=2)
      {
   printf("0 = Move Mass Inwards\n");
      printf("1 = Move Mass Outwards\n");

      scanf("%d",&f);
   }

            if (f==0)
      {
      y = 32;
//    printf("y = 32\n");
      }
            else
      {
            y = 48;
//      printf("y = 48\n");
            }
w = 4;
u = 16;

printf("Type number of steps\n");
scanf("%d",&x);
printf("you chose no of steps: %d \n",x);
printf("Type steps per second\n");
```

```
scanf("%lf",&z);
printf("you chose no of steps: %lf \n",z);

s = 0.5/z;

outp(port,value);

outp(port_2,value);


printf("Running...\n");

//for(i=1;i<=20;++i){
//    printf("\n");
//    }

      r = y & 21;
for (i=x;i>=0;i=i-1)
      {
//    x = x - 1;

      outp(base+5,r);

      Delay(s);

      outp(base+5,y);

    Delay(s);

//    printf("%d\n",i);
/*    lmt1=inp(port_3);
      if ((lmt1 & w) == 0)
      {
      y = u ^ y;
      r = y & 0x15;
            while((lmt1 & w) > 0)
         {
         outp(base+5,r);
         Delay(0.3);
         outp(base+5,y);
         Delay(0.3);
         lmt1=inp(base+4);
         printf("Motor at limit switch.\n");
         x=0;
         }
*/      }


printf("test complete\n");
}
```

Appendix C CVI Program for the feedback control system

```
/*********************************************************************
*
* Controller program:
*    DAQ.c – Chris Ting
*
* Description:
*    1) Read a waveform from one analog input channel using internal
*       timing (uses low-level NI-DAQ functions)
*
*    2) Process samples of this waveform and performs filtering and FFT
*       algorithms to it.
*    3) Send and output signal to the controller step motor based on the above
*       results.
*
* Program Category:
*    AI, AO
*
* List of key parameters:
*    iDAQstopped
*
*
* List of NI-DAQ Functions used in this example:
*    DAQ_Rate, DAQ_Start, NIDAQErrorHandler, DAQ_Check, NIDAQYield,
*     DAQ_VScale, DAQ_Clear, NIDAQPlotWaveform
*
*
* Pin Connection Information:
*    Connect the analog signal to AI channel 1. The default analog
*     input mode for the DAQ device will be used. Connect the 8255 card to
*     ISA port. Use slot 2 on control card.
*
*********************************************************************/
/*
 * Includes:
 */
#include <stdio.h>
#include "nidaqex.h"
#include "tryagain.h"
#include <dataacq.h>
#include <userint.h>
#include <utility.h>
#include <easyio.h>
#include <cvirte.h>
#include <analysis.h>

/*
     * Local Variable Declarations:
     */

      static int xx=1,i;
    i16 iStatus = 0;
    i16 iRetVal = 0;
    i16 iDevice = 1;
    i16 iChan = 1;
    i16 iGain = 1;
    f64 dSampRate = 4000.0;
    u32 ulCount = 512;
    f64 dGainAdjust = 1.0;
    f64 dOffset = 0.0;
```

```
    i16 iUnits = 0;
    i16 iSampTB = 0;
    u16 uSampInt = 0;
    static i16 piBuffer[2048] = {0};
    i16 iDAQstopped = 0;
    u32 ulRetrieved = 0;
    static f64 pdVoltBuffer[2048] = {0.0};
    static f64 VoltBufferA[2048] = {0.0};
    static f64 VoltBufferB[2048] = {0.0};
    static f64 VoltBufferC[2048] = {0.0};
    static f64 VoltBufferD[2048] = {0.0};
    static double spectrum[2048] = {0.0};
    static double spectrumA[2048] = {0.0};
    static double spectrumB[2048] = {0.0};
    static double freqspace;
    double BufferA,BufferB;
    i16 iIgnoreWarning = 0;
    i16 iYieldON = 1;
      static int mainpnl;
      void *callbackData;
      double sec=0.1;
      double BufferSum;
      double BufferAverage;
      double rmsval;
      double BufferC;
      double ModBuffer;
      int points=2048;
      double SpecMaxValue;
      int SpecMaxIndex;
      double SpecMinValue;
      int SpecMinIndex;
      double SpecMaxIndex2;
      double DisplaceVolt;

      // stepper motor variables
      const static base = 432;
    int x,y,w,lmt1,u,f=3,r,value=144,port=435,port_2=439,port_3=436 ;
    long double z,s;
      int dirflag=0;
      int loopflag=0;

/*
 * Main:
 */

void main(int argc, char *argv[])
{

    /* Convert sample rate (S/sec) to appropriate timebase and sample
     interval values. */

    iStatus = DAQ_Clear(iDevice);
    iStatus = DAQ_Rate(dSampRate, iUnits, &iSampTB, &uSampInt);


    /* start user interface */

      mainpnl = LoadPanel (0, "tryagain.uir", MAINPNL);

      SetInputMode(mainpnl, MAINPNL_START, 1);
    SetInputMode(mainpnl, MAINPNL_STOP,  0);
    SetCtrlAttribute (mainpnl, MAINPNL_TIMER, ATTR_ENABLED, 0);
```

```
    DisplayPanel (mainpnl);
    RunUserInterface ();

}


    /* Acquire data from a single channel */

CVICALLBACK Start (int panel, int control, int event,
        void *callbackData, int eventData1, int eventData2 )
{
    switch (event) {
        case EVENT_COMMIT:

            SetInputMode(mainpnl, MAINPNL_START, 0);
            SetInputMode(mainpnl, MAINPNL_STOP,  1);

            SetCtrlAttribute (mainpnl, MAINPNL_TIMER,  ATTR_ENABLED,1);
        case EVENT_TIMER_TICK:


      iStatus = DeleteGraphPlot (mainpnl, MAINPNL_TIMEGRAPH, -1,
VAL_DELAYED_DRAW);

            iStatus = DAQ_Start(iDevice, iChan, iGain, piBuffer, ulCount,
                  iSampTB, uSampInt);
            iRetVal = NIDAQErrorHandler(iStatus, "DAQ_Start", iIgnoreWarning);
      while ((iDAQstopped != 1) && (iStatus == 0))
      {

         /* Loop until all acquisition is complete.    */

            iStatus = DAQ_Check(iDevice, &iDAQstopped, &ulRetrieved);

            iRetVal = NIDAQYield(iYieldON);
      }


    iRetVal = NIDAQErrorHandler(iStatus, "DAQ_Check", iIgnoreWarning);


    iStatus = DAQ_VScale(iDevice, iChan, iGain, dGainAdjust, dOffset,
     ulCount, piBuffer, pdVoltBuffer);

    iRetVal = NIDAQErrorHandler(iStatus, "DAQ_VScale",
     iIgnoreWarning);

      /* Plot acquired data */

      iStatus = PlotY (mainpnl, MAINPNL_TIMEGRAPH, pdVoltBuffer, ulCount,
WFM_DATA_F64,
                   VAL_THIN_LINE, VAL_EMPTY_SQUARE, VAL_SOLID, 1, VAL_RED);
    iStatus = Mean(pdVoltBuffer, 512, &DisplaceVolt);



    Delay(sec);

      iStatus = RMS (pdVoltBuffer, ulCount, &rmsval);

      if (xx==1)
```

```
      {
       BufferA=rmsval;

       xx=0;
       }
       else
       {
       BufferB=rmsval;

        xx=1;
        }

      BufferC=BufferA-BufferB;
      ModBuffer=sqrt(BufferC*BufferC);

      SetCtrlVal (mainpnl, MAINPNL_METER, ModBuffer);
      SetCtrlVal (mainpnl, MAINPNL_DISPLACEVOLT, DisplaceVolt);

      iStatus = DAQ_Clear(iDevice);

    /* Calculate Power Spectrum and Plot Frequency Graph */


      AutoPowerSpectrum (pdVoltBuffer, points, (1/dSampRate), spectrum,
                                    &freqspace);

    for (i=0; i<(points/2); i++) {
                             spectrum[i] = 20*(log10(spectrum[i]));
                        }

      MaxMin1D (spectrum, points/2, &SpecMaxValue, &SpecMaxIndex,
                    &SpecMinValue, &SpecMinIndex);

      SpecMaxIndex2 = SpecMaxIndex*2;

      SetCtrlVal (mainpnl, MAINPNL_SPECMAXINDEX, SpecMaxIndex2);
      SetCtrlVal (mainpnl, MAINPNL_SPECMAXVALUE, SpecMaxValue);

    SetAxisRange (mainpnl, MAINPNL_FREQGRAPH, VAL_NO_CHANGE, 0.0, 400.0,
                                        VAL_NO_CHANGE, -90, 50.00);
    DeleteGraphPlot (mainpnl, MAINPNL_FREQGRAPH, -1, VAL_DELAYED_DRAW);


    PlotWaveform (mainpnl, MAINPNL_FREQGRAPH, spectrum, points,
                               VAL_DOUBLE, 1.0, 0.0, 0.0, freqspace,
VAL_THIN_LINE,
                               VAL_EMPTY_SQUARE, VAL_SOLID, 1, VAL_RED);


 /*   if (dirflag==1){

        if (i>0){
            r = y & 21;
            for (loopflag=500;loopflag>=0;loopflag=loopflag-1){
                  outp(base+5,r);

                  Delay(s);

                  outp(base+5,y);

                  Delay(s);
                  i=i-1;
```

```
                }
            }
            if (i=0){
                        x=0;
                        dirflag=0;
                        }
      }
    if (dirflag==2){

        if (i>0){
            r = y & 21;
            for (loopflag=500;loopflag>=0;loopflag=loopflag-1){
                  outp(base+5,r);

                  Delay(s);

                  outp(base+5,y);

                  Delay(s);
                  i=i-1;

            }
        }
        if (i=0){
                  x=0;
                  dirflag=0;
                  }
    }  */
        break;
            case EVENT_RIGHT_CLICK:
            MessagePopup ("Start Data Acquisition",
                          "Begins signal acquisition and processing.");
            break;
        break;
    }
    return 0;

}


CVICALLBACK Quit (int panel, int control, int event,
        void *callbackData, int eventData1, int eventData2)
{
    switch (event) {
        case EVENT_COMMIT:


            QuitUserInterface (0);
            break;
        case EVENT_RIGHT_CLICK:
            MessagePopup ("Quit",
                          "Quits the program.");
            break;
    }
    return 0;
}

int CVICALLBACK Stop (int panel, int control, int event,
        void *callbackData, int eventData1, int eventData2)
{
    switch (event) {
```

```
        case EVENT_COMMIT:
            SetCtrlAttribute (mainpnl, MAINPNL_TIMER, ATTR_ENABLED, 0);
            SetInputMode(mainpnl, MAINPNL_START, 1);
            SetInputMode(mainpnl, MAINPNL_STOP,  0);
            break;
        case EVENT_RIGHT_CLICK:
            MessagePopup ("Stop Data Acquisition",
                          "Disables signal acquisition and processing.");
            break;
    }

    return 0;
}


CVICALLBACK StepNumber (int panel, int control, int event,
        void *callbackData, int eventData1, int eventData2)
{
      switch (event) {
        case EVENT_COMMIT:
            //GetCtrlVal (mainpnl, MAINPNL_STEPNUMBER, &x);
            break;
        case EVENT_RIGHT_CLICK:
            MessagePopup ("Set the Number of Steps",
                          "Sets the number of steps for the motor to turn");
            break;
    }
    return 0;
}


CVICALLBACK StepRate (int panel, int control, int event,
        void *callbackData, int eventData1, int eventData2)
{
      switch (event) {
        case EVENT_COMMIT:
            //GetCtrlVal (mainpnl, MAINPNL_STEPRATE, &z);
            break;
        case EVENT_RIGHT_CLICK:
            MessagePopup ("Set the StepRate",
                          "Sets the number of steps per second.");
            break;
    }
    return 0;
}


CVICALLBACK Outwards (int panel, int control, int event,
        void *callbackData, int eventData1, int eventData2)
{
      //switch (event) {
      //case EVENT_TIMER_TICK:

      GetCtrlVal (mainpnl, MAINPNL_STEPNUMBER, &x);
      GetCtrlVal (mainpnl, MAINPNL_STEPRATE, &z);
      y = 48;
    w = 4;
    u = 16;

    s = 0.5/z;
    outp(port_2,value);
    //dirflag=1;
```

```
    r = y & 21;

      for (i=x;i>=1;i=i-1)
            {
          outp(base+5,r);

          Delay(s);

      outp(base+5,y);

        Delay(s);
        x=0;
        }

    //break;
      //}
      SetCtrlVal (mainpnl, MAINPNL_STEPNUMBER, i);
      return 0;
}


CVICALLBACK Inwards (int panel, int control, int event,
        void *callbackData, int eventData1, int eventData2)
{
    //switch (event) {
    //case EVENT_TIMER_TICK:

    GetCtrlVal (mainpnl, MAINPNL_STEPNUMBER, &x);
    GetCtrlVal (mainpnl, MAINPNL_STEPRATE, &z);
    y = 32;
    w = 4;
    u = 16;

    s = 0.5/z;
    outp(port_2,value);
    //dirflag=2;

    r = y & 21;


      for (i=x;i>=1;i=i-1)
          {
          outp(base+5,r);

          Delay(s);

      outp(base+5,y);

        Delay(s);

        }


      //break;
      //}
      SetCtrlVal (mainpnl, MAINPNL_STEPNUMBER, i);
      return 0;
}
/* End of program */
```

Appendix D Illustrations

Figure C1 – First prototype

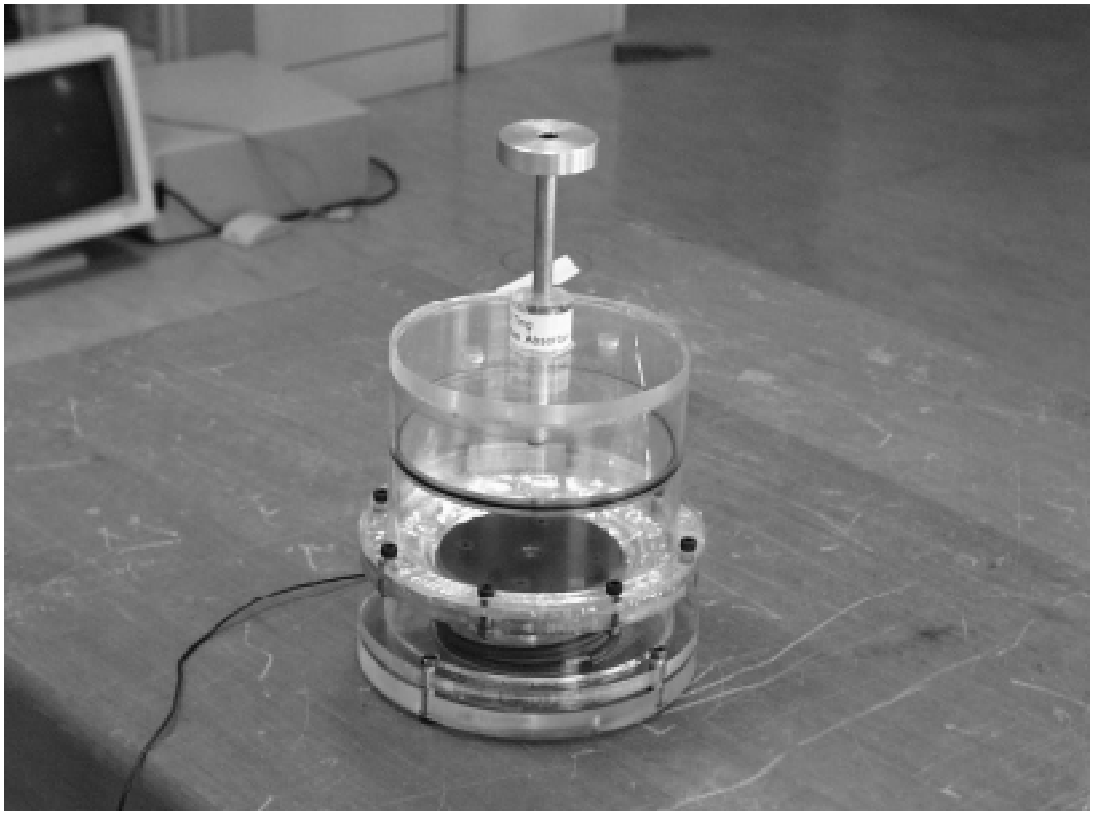

Figure C2 – Second Prototype

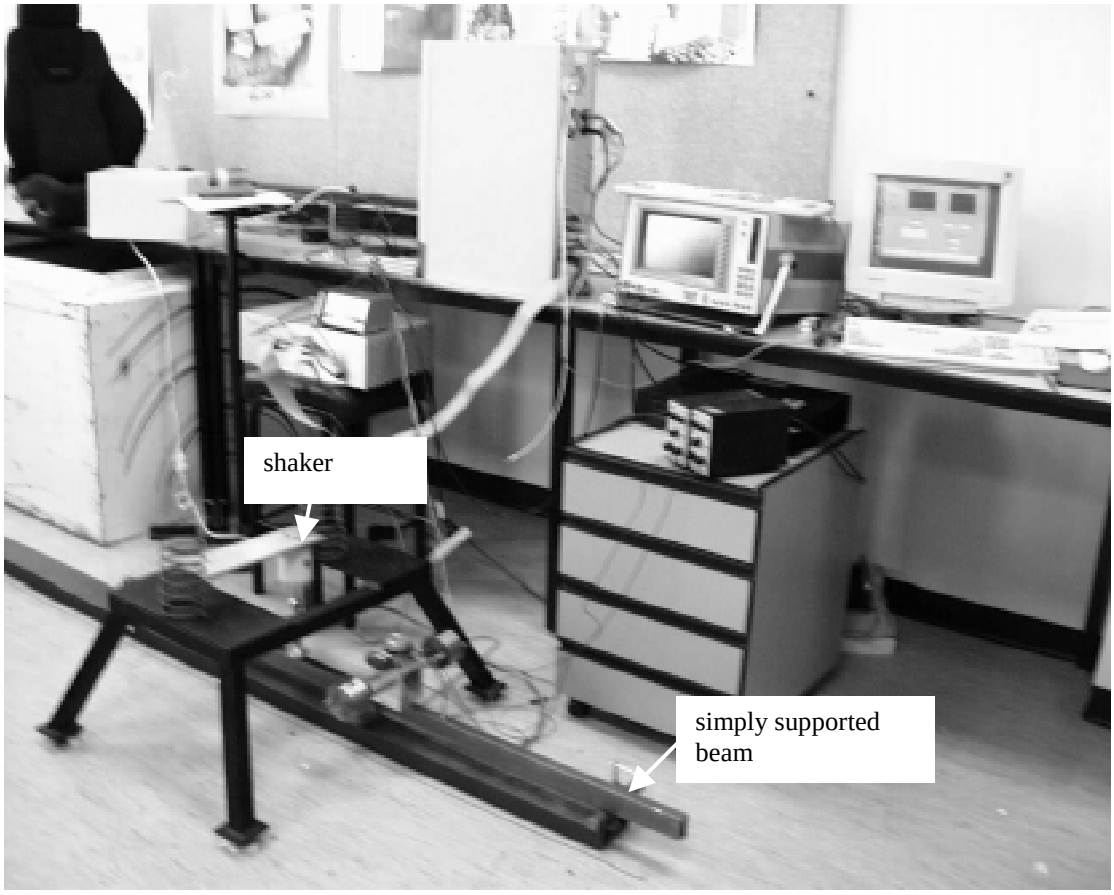

Figure C3 – Experimental setup 2

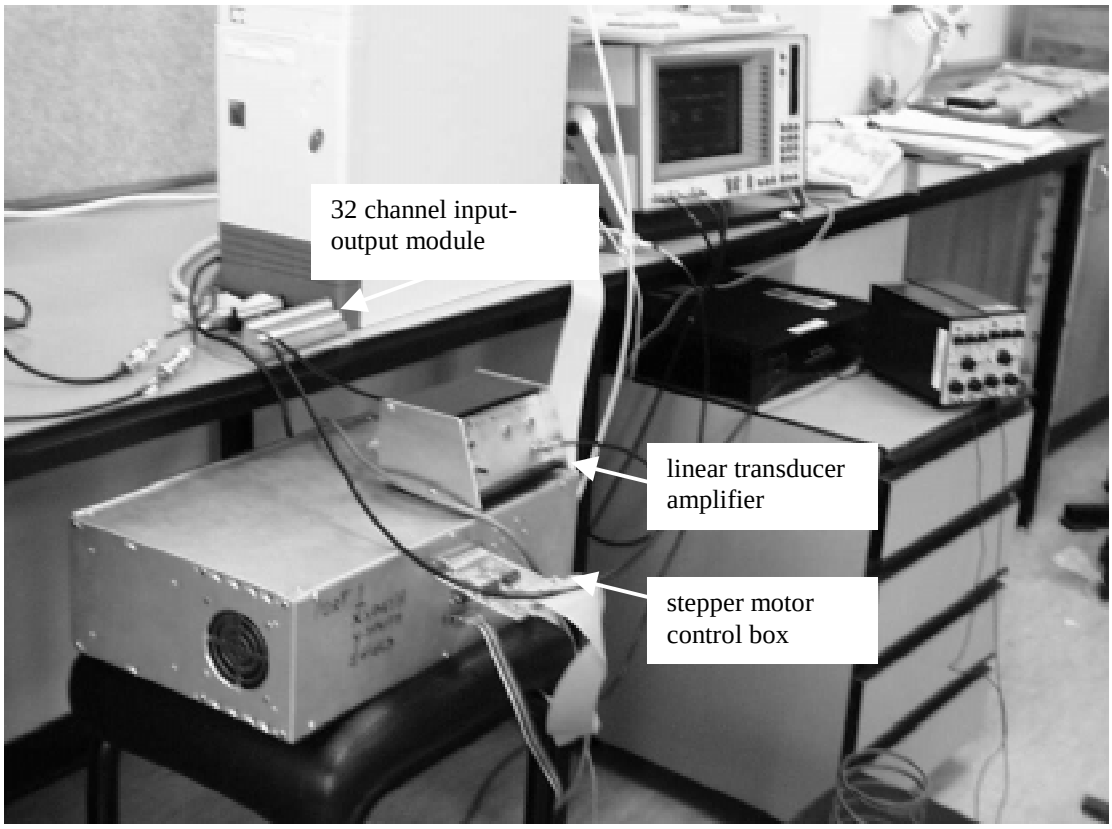

Figure C4 – Controller and transducer box

REFERENCES

Bernhard, R. J., Hall, H. R., Jones, J. D., ”Adaptive-Passive noise control”, *Inter-Noise 92*, 427-430.

Bies, D. A., Hansen, C. H. (1996), *Engineering Noise Control – Theory and Practice*, Chapman and Hall, London.

Broch, J. T. (1975), *The Application of Bruel and Kjaer Measuring Systems to Mechanical Vibration and Shock Measurements*, Bruel and Kjaer Publishing.

Bruner, A. M., Belvin, W. K., Horta, L. G., Juang, J. N. (1992), “Active Vibration Absorber for the CSI Evolutionary Model: Design and Experimental Results”, *Journal of Guidance, Control, and Dynamics*, Vol. 15, No. 5, Sept, 1253–1257.

Buzdugan, G. (1986), *Vibration Measurement*, Dordrecht, Boston.

Den Hartog, J. P. (1956), *Mechanical Vibrations* (4th edition) Mc Graw-Hill, New York.

Ewins, D. J. (1984), *Modal Testing – Theory and Practice*, Letchworth, Hertfordshire, England.

Flannelly, W. G. (1963), “Dynamic Antiresonant Vibration Isolator,” Kaman Aircraft Corporation, Bloomfield, Conn., Report RN63-1, Nov.

Flannelly, W. G., Jones, R. (1978), “Application of Dynamic Antiresonant Vibration Isolator to Helicopter Vibration Control”, US Naval Research Lab., *Shock and Vibration Bulletin*, Vol. 37,

Jan, 63-81.

Graf, P. I., Shoureshi, R., Stevens, R. W., Houston T. L. (1987), "Implementation of Adaptive Hydraulic Mounts", *SAE* Paper No. 870634.

Harris, C., Crede, C. (1961), *Shock and Vibration Handbook* (vol. 1), Mc Graw-Hill, New York.

Hunt, J. B. (1979), *Dynamic Vibration Absorbers* Mechanical Engineering Publications Ltd, London.

Korenev, B. G., Reznikov, L. M.(1993), *Dynamic Vibration Absorbers- Theory and Technical Applications*, Wiley, New York.

Jones, R. (1971), "A Full-Scale Experimental Study of Helicopter Rotor Isolation Using the Dynamic Antiresonant Vibration Isolator", Kaman Aerospace Corp., Bloomfield, Conn.

Juang, J. N. (1984),"Optimal Design of a Passive Vibration Absorber for a Truss Beam", *Journal of Guidance, Control and Dynamics*, Vol. 7, No. 6, Nov.

Lamancusa J. S. (1987), "An Actively Tuned, Passive Muffler System For Engine Silencing", *Noise-Con 87*, 313-318.

Lee-Glauser, G., Juang, J.-N., Sulla, J. L. (1995), "Optimal Active Vibration Absorber: Design and Experimental Results", *Journal of Vibration and Acoustics*, Vol. 117.

References

Mc Callion, H. (1973), *Vibration of Linear Mechanical Systems*, Longman Group Ltd, London, 96–110.

Nestorides, E. J. (1958), *A Handbook on Torsional Vibration*, Cambridge University Press, London.

Nishimura, H., Yoshida, K., Shimogo, T. (1990), "Optimal Active Dynamic Vibration Absorber for Multi-Degree-of-Freedom Systems", *JSME International Journal*, Vol. 33, No. 4, Ser. III, 513.

Nonami, K., Hidekazu, N., Weimin, C. (1994), "Disturbance Cancellation Control for Vibration of Multi-Degree-of-Freedom Systems", *JSME International Journal*, Vol. 37, No.1, Ser. C.

Plunket, R. (1958), *Colloquium on Mechanical Impedance Methods*, ASME Annual Meeting, chapter V.

Rita, A. D., Mc Garvey, J. H., Jones, R. (1978),"Helicopter Rotor Isolation Evaluation Using the Dynamic Antiresonant Vibration Isolator", *Journal of the American Helicopter Society*, Vol. 23,No. 1, Jan, 22-29.

Rockwell, T. H. (1965), "Investigation of Structure-Borne Active Vibration Dampers", *Journal of Acoustical Society America*, Vol. 38, 623-8.

Ryan, M.W., Franchek, M. A., Bernhard, R. (1994), "Adaptive-Passive Vibration Control of Single Frequency Excitations Applied to Noise Control", *Noise-Con 94*, 461-466.

References

Seto, W.(1964), *Schaum's outline of Theory and Problems of Mechanical* Vibrations, Mc Graw Hill, Singapore, Chapt. 5, 128-150.

Snowdon, J. C. (1968), "*Vibration of Shock in Damped Mechanical Systems*", Wiley, New York.

Thomson, W. T. (1993), *Theory of Vibration with Applications*, Prentice Hall, 281-286.

Tse, S. F., Morse, I. E., Hinkle, R. T. (1978), *Mechanical Vibrations – Theory and Applications*, Allyn and Bacon Inc, Sydney, 272-284.

Von Flotow, A., Beard, A., Bailey, D., "Adaptive Tuned Vibration Absorbers: Tuning Laws, Tracking Agility, Sizing, and Physical Implementations", *Noise-Con 94*, 437-454.

Wang, K., Kim, Y., Shea, B. (1994), "Structural vibration control via electrorheological-fluid-based actuators with adaptive viscous and frictional damping", *Journal of Sound and Vibration*, Vol 177, 227-237.

Wang, B. P., Kitis, L., Pilkey, W. D., Palazzolo, A. (1985), "Synthesis of Dynamic Vibration Absorbers", *Journal of Vibration, Stress and Reliability in Design*, Vol. 107, Apr, 161.

Yoshida, K., Shimogo, T., Nishimura, H. (1988), "Optimal Control of Random Vibration by the Use of Active Dynamic Absorber", *Trans. JSME International Journal*, Series III, Vol. 31, No. 2 .